sensitive assay to identify chemopreventive phytochemicals, because the Western blots in Figure 4 suggest that a 10-fold increase of the protein can be readily achieved.

Significant variations in the amounts and the types of glucosinolates in different broccoli strains appear to exist (7–9). Because this will result in distinct ITCs being generated by myrosinase from different broccoli strains, these differences in glucosinolate content will also influence the level of induction that can be achieved in the host and also possibly the sensitivity to cell-cycle arrest. The significance of variation in the glucosinolate content of cruciferous vegetables in terms of antioxidant and detoxication gene induction and stimulation of cell-cycle arrest and apoptosis warrants further study.

ACKNOWLEDGMENT

We thank Jed Fahey for valuable constructive criticism of this work during the AICR conference and for pointing out the confounding effects of epithiospecifier protein on glucosinolate degradation.

LITERATURE CITED

1. Block, G., Patterson, B. & Subar, A. (1992) Fruit, vegetables, and cancer prevention: a review of the epidemiological evidence. Nutr. Cancer 18: 1–29.

2. Verhoeven, D.T.H., Verhagen, H., Goldbohm, R. A., van den Brandt, P. A. & van Poppel, G. (1997) A review of mechanisms underlying anticarcinogenicity by brassica vegetables. Chem. Biol. Interact. 103: 79–129.

3. Van Poppel, G., Verhoeven, D. T., Verhagen, H. & Goldbohm, R. A. (1999) Brassica vegetables and cancer prevention. Epidemiology and mechanisms. Adv. Exp. Med. Biol. 472: 159–168.

4. Steinkellner, H., Rabot, S., Freywald, C., Nobis, E., Scharf, G., Chabicovsky, M., Knasmüller, S. & Kassie, F. (2001) Effects of cruciferous vegetables and their constituents on drug metabolising enzymes involved in the bioactivation of DNA-reactive dietary carcinogens. Mutat. Res. 480–481: 285–297.

5. Talalay, P. & Fahey, J. W. (2001) Phytochemicals from cruciferous plants protect against cancer by modulating carcinogen metabolism. J. Nutr. 131: 3027S–3033S.

6. Conaway, C. C., Yang, Y.-M. & Chung, F.-L. (2002) Isothiocyanates as cancer chemopreventive agents: their biological activities and metabolism in rodents and humans. Curr. Drug Metab. 3: 233–255.

7. Fenwick, G. R., Heaney, R. K. & Mullin, W. J. (1983) Glucosinolates and their breakdown products in food and food plants. CRC Crit. Rev. Food Sci. Nutr. 18: 123–201.

8. Fahey, J. W., Zalcmann, A. T. & Talalay, P. (2001) The chemical diversity and distribution of glucosinolates and isothiocyanates among plants. Phytochemistry 56: 5–51.

9. Matusheski, N. V., Juvik, J. A. & Jeffery, E. H. (2004) Heating decreases epithiospecifier protein activity and increases sulforaphane formation in broccoli. Phytochemistry 65: 1273–1281.

10. Zhang, Y., Talalay, P., Cho, C. G. & Posner, G. H. (1992) A major inducer of anticarcinogenic protective enzymes from broccoli: isolation and elucidation of structure. Proc. Natl. Acad. Sci. U.S.A. 89: 2399–2403.

11. Tawfiq, N., Heaney, R. K., Plumb, J. A., Fenwick, G. R., Musk, S.R.R. & Williamson, G. (1995) Dietary glucosinolates as blocking agents against carcinogenesis: glucosinolate breakdown products assessed by induction of quinone reductase activity in murine hepa1c1c7 cells. Carcinogenesis 16: 1191–1194.

12. Kelly, V. P., Ellis, E. M., Manson, M. M., Chanas, S. A., Moffat, G. J., McLeod, R., Judah, D. J., Neal, G. E. & Hayes, J. D. (2000) Chemoprevention of aflatoxin B_1 hepatocarcinogenesis by coumarin, a natural benzopyrone that is a potent inducer of AFB_1-aldehyde reductase, the glutathione S-transferase A5 and P1 subunits, and NAD(P)H:quinone oxidoreductase in rat liver. Cancer Res. 60: 957–969.

13. Nakamura, Y., Morimitsu, Y., Uzu, T., Ohigashi, H., Murakami, A., Naito, Y., Nakagawa, Y., Osawa, T. & Uchida, K. (2000) A glutathione S-transferase inducer from papaya: rapid screening, identification and structure-activity relationship of isothiocyanates. Cancer Lett. 157: 193–200.

14. Bonnesen, C., Eggleston, I. M. & Hayes, J. D. (2001) Dietary indoles and isothiocyanates that are generated from cruciferous vegetables can both stimulate apoptosis and confer protection against DNA damage in human colon cell lines. Cancer Res. 61: 6120–6130.

15. Brooks, J. D., Paton, V. G. & Vidanes, G. (2001) Potent induction of phase 2 enzymes in human prostate cells by sulforaphane. Cancer Epidemiol. Biomark. Prev. 10: 949–954.

16. Morimitsu, Y., Nakagawa, Y., Haayashi, K., Fujii, H., Kumagai, T., Nakamura, Y., Osawa, T., Horio, F., Itoh, K., et al. (2002) A sulforaphane analogue that potently activates the Nrf2-dependent detoxification pathway. J. Biol. Chem. 277: 3456–3463.

17. Jiang, Z.-Q., Chen, C., Yang, B., Hebbar, V. & Kong, A.-N.T. (2003) Differential responses from seven mammalian cell lines to the treatments of detoxifying enzyme inducers. Life Sci. 72: 2243–2253.

18. Fahey, J. W., Haristoy, X., Dolan, P. M., Kensler, T. W., Scholtus, I., Stephenson, K. K., Talalay, P. & Lozniewski, A. (2002) Sulforaphane inhibits extracellular, intracellular, and antibiotic-resistant strains of *Helicobacter pylori* and prevents benzo[a]pyrene-induced stomach tumors. Proc. Natl. Acad. Sci. U.S.A. 99: 7610–7615.

19. McMahon, M., Itoh, K., Yamamoto, M., Chanas, S. A., Henderson, C. J., McLellan, L. I., Wolf, C. R., Cavin, C. & Hayes, J. D. (2001) The cap'n'collar basic leucine zipper transcription factor Nrf2 (NF-E2 p45-related factor 2) controls both constitutive and inducible expression of intestinal detoxification and glutathione biosynthetic enzymes. Cancer Res. 61: 3299–3307.

20. Thimmulappa, R. K., Mai, K. H., Srisuma, S., Kensler, T. W., Yamamoto, M. & Biswal, S. (2002) Identification of Nrf2-regulated genes induced by the chemopreventive agent sulforaphane by oligonucleotide microarray. Cancer Res. 62: 5196–5203.

21. Hayes, J. D. & McLellan, L. I. (1999) Glutathione and glutathione-dependent enzymes represent a co-ordinately regulated defence against oxidative stress. Free Rad. Res. 31: 273–300.

22. Motohashi, H., O'Connor, T., Katsuoka, F., Engel, J. D. & Yamamoto, M. (2002) Integration and diversity of the regulatory network composed of Maf and CNC families of transcription factors. Gene 294: 1–12.

23. Nguyen, T., Sherratt, P. J., Huang, H. C., Yang, C. S. & Pickett, C. B. (2003) Increased protein stability as a mechanism that enhances Nrf2-mediated transcriptional activation of the antioxidant response element—degradation of Nrf2 by the 26 S proteasome. J. Biol. Chem. 278: 4536–4541.

24. Itoh, K., Wakabayashi, N., Katoh, Y., Ishii, T., O'Connor, T. & Yamamoto, M. (2003) Keap1 regulates both cytoplasmic-nuclear shuttling and degradation of Nrf2 in response to electrophiles. Genes Cells 8: 379–391.

25. McMahon, M., Itoh, K., Yamamoto, M. & Hayes, J. D. (2003) Keap1-dependent proteasomal degradation of transcription factor Nrf2 contributes to the negative regulation of antioxidant response element-driven gene expression. J. Biol. Chem. 278: 21592–21600.

26. McMahon, M., Thomas, N., Itoh, K., Yamamoto, M. & Hayes, J. D. (2004) Redox-regulated turnover of Nrf2 is determined by at least two separate protein domains, the redox-sensitive Neh2 degron and the redox-insensitive Neh6 degron. J. Biol. Chem. 279: 31556–31567.

27. Wakabayashi, N., Dinkova-Kostova, A. T., Holtzclaw, W. D., Kang, M. I., Kobayashi, A., Yamamoto, M., Kensler, T. W. & Talalay, P. (2004) Protection against electrophile and oxidant stress by induction of the phase 2 response: fate of cysteines of the Keap1 sensor modified by inducers. Proc. Natl. Acad. Sci. U.S.A. 101: 2040–2045.

28. Nguyen, T., Sherratt, P. J. & Pickett, C. B. (2003) Regulatory mechanisms controlling gene expression mediated by the antioxidant response element. Annu. Rev. Pharmacol. Toxicol. 43: 233–260.

29. Nioi, P., McMahon, M., Itoh, K., Yamamoto, M. & Hayes, J. D. (2003) Identification of a novel Nrf2-regulated antioxidant response element in the mouse NAD(P)H:quinone oxidoreductase 1 gene; reassessment of the ARE consensus sequence. Biochem. J. 374: 337–348.

30. Jowsey, I. R., Jiang, Q., Itoh, K., Yamamoto, M. & Hayes, J. D. (2003) Expression of the aflatoxin B_1-8,9-epoxide-metabolizing murine glutathione S-transferase A3 subunit is regulated by the Nrf2 transcription factor through an antioxidant response element. Mol. Pharmacol. 64: 1018–1028.

31. Hayes, J. D., Chanas, S. A., Henderson, C. J., McMahon, M., Sun, C., Moffat, G. J., Wolf, C. R. & Yamamoto, M. (2000) The Nrf2 transcription factor contributes both to the basal expression of glutathione S-transferases in mouse liver and to their induction by the chemopreventive synthetic antioxidants, butylated hydroxyanisole and ethoxyquin. Biochem. Soc. Trans. 28: 33–41.

32. Nioi, P. & Hayes, J. D. (2004) Contribution of NAD(P)H:quinone oxidoreductase 1 to protection against carcinogenesis, and regulation of its gene by the Nrf2 basic-region leucine zipper and the Arylhydrocarbon receptor basic helix-loop-helix transcription factors. Mutat. Res. 555: 149–171.

33. Itoh, K., Chiba, T., Takahashi, S., Ishii, T., Igarashi, K., Katoh, Y., Oyake, T., Hayashi, N., Satoh, K., et al. (1997) An Nrf2/small Maf heterodimer mediates the induction of phase II detoxifying enzyme genes through antioxidant response elements. Biochem. Biophys. Res. Commun. 236: 313–322.

34. Chanas, S. A., Jiang, Q., McMahon, M., McWalter, G. K., McLellan, L. I., Elcombe, C. R., Henderson, C. J., Wolf, C. R., Moffat, G. J., et al. (2002) Loss of the Nrf2 transcription factor causes a marked reduction in constitutive and inducible expression of the glutathione S-transferase *Gsta1*, *Gsta2*, *Gstm1*, *Gstm2*, *Gstm3* and *Gstm4* genes in the livers of male and female mice. Biochem. J. 365: 405–416.

35. Dinkova-Kostova, A. T., Fahey, J. W. & Talalay, P. (2004) Chemical structures of inducers of nicotinamide quinone oxidoreductase 1 (NQO1). Methods Enzymol. 382: 423–448.

36. Barillari, J., Gueyrard, D., Rollin, P. & Iori, R. (2001) *Barbarea verna* as a source of 2-phenylethyl glucosinolate, precursor of cancer chemopreventive phenylethyl isothiocyanate. Fitoterapia 72: 760–764.

37. Nastruzzi, C., Cortesi, R., Esposito, E., Menegatti, E., Leoni, O., Iori, R. & Palmieri, S. (2000) In vitro antiproliferative activity of isothiocyanates and nitriles generated by myrosinase-mediated hydrolysis of glucosinolates from seeds of cruciferous vegetables. J. Agric. Food Chem. 48: 3572–3575.

38. Mellon, F. A., Bennett, R. N., Holst, B. & Williamson, G. (2002) Intact glucosinolate analysis in plant extracts by programmed cone voltage electrospray

LC/MS: performance and comparison with LC/MS/MS methods. Anal. Biochem. 306: 83–91.

39. Tiemann, F. & Deppert, W. (1994) Immortalization of BALB/c mouse embryo fibroblasts alters SV40 large T-antigen interactions with the tumor suppressor p53 and results in a reduced SV40 transformation-efficiency. Oncogene 9: 1907–1915.

40. Dinkova-Kostova, A. T., Massiah, M. A., Bozak, R. E., Hicks, R. J. & Talalay, P. (2001) Potency of Michael reaction acceptors as inducers of enzymes that protect against carcinogenesis depends on their reactivity with sulfhydryl groups. Proc. Natl. Acad. Sci. U.S.A. 98: 3404–3409.

41. Singh, S. V., Herman-Antosiewicz, A., Singh, A. V., Lew, K. L., Srivastava, S. K., Kamath, R., Brown, K. D., Zhang, L. & Baskaran, R. (2004) Sulforaphane-induced G2/M phase cell cycle arrest involves checkpoint kinase 2-mediated phosphorylation of cell division cycle 25C. J. Biol. Chem. 279: 25813–25822.

42. Petroski, R. J. & Tookey, H. L. (1982) Interactions of thioglucoside glucohydrolase and epithiospecifier protein of cruciferous plants to form 1-cyanoepithioalkanes. Phytochemistry 21: 1903–1905.

43. Fahey, J. W., Zhang, Y. & Talalay, P. (1997) Broccoli sprouts: an exceptionally rich source of inducers of enzymes that protect against chemical carcinogens. Proc. Natl. Acad. Sci. U.S.A. 94: 10367–10372.

44. Andorfer, J. H., Tchaikovskaya, T. & Listowsky, I. (2004) Selective expression of glutathione S-transferase genes in the murine gastrointestinal tract in response to dietary organosulfur compounds. Carcinogenesis 25: 359–367.

45. Wild, A. C., Moinova, H. R. & Mulcahy, R. T. (1999) Regulation of gamma-glutamylcysteine synthetase subunit gene expression by the transcription factor Nrf2. J. Biol. Chem. 274: 33627–33636.

46. Kang, Y. H. & Pezzuto, J. M. (2004) Induction of quinone reductase as a primary screen for natural product anticarcinogens. Methods Enzymol. 382: 380–414.

Available online at www.sciencedirect.com

SCIENCE DIRECT

Free Radical Biology & Medicine 38 (2005) 325–343

www.elsevier.com/locate/freeradbiomed

Original Contribution

Gene expression profiling of NRF2-mediated protection against oxidative injury

Hye-Youn Cho[a,b,*], Sekhar P. Reddy[a], Andrea DeBiase[c], Masayuki Yamamoto[d], Steven R. Kleeberger[a,b]

[a]*Department of Environmental Health Sciences, Johns Hopkins University Bloomberg School of Public Health, Baltimore, MD 21205, USA*
[b]*Laboratory of Respiratory Biology, National Institute of Environmental Health Sciences, National Institutes of Health, Research Triangle Park, NC 27709, USA*
[c]*Children's National Medical Center, George Washington University, Washington, DC 20010, USA*
[d]*Institute of Basic Medical Sciences and Center for Tsukuba, Advanced Research Alliance, University of Tsukuba, Tennoudai, Tsukuba 305, Japan*

Received 14 May 2004; accepted 6 October 2004
Available online 12 November 2004

Abstract

Nuclear factor E2 p45-related factor 2 (NRF2) contributes to cellular protection against oxidative insults and chemical carcinogens via transcriptional activation of antioxidant/detoxifying enzymes. To understand the molecular basis of NRF2-mediated protection against oxidative lung injury, pulmonary gene expression profiles were characterized in *Nrf2*-disrupted ($Nrf2^{-/-}$) and wild-type ($Nrf2^{+/+}$) mice exposed to hyperoxia or air. Genes expressed constitutively higher in $Nrf2^{+/+}$ mice than in $Nrf2^{-/-}$ mice included antioxidant defense enzyme and immune cell receptor genes. Higher basal expression of heat shock protein and structural genes was detected in $Nrf2^{-/-}$ mice relative to $Nrf2^{+/+}$ mice. Hyperoxia enhanced expression of 175 genes (≥ twofold) and decreased expression of 100 genes (≥50%) in wild-type mice. Hyperoxia-induced upregulation of many well-known/new antioxidant/defense genes (e.g., *Txnrd1*, *Ex*, *Cp-2*) and other novel genes (e.g., *Pkc-α*, *Tcf-3*, *Ppar-γ*) was markedly greater in $Nrf2^{+/+}$ mice than in $Nrf2^{-/-}$ mice. In contrast, induced expression of genes encoding extracellular matrix and cytoskeletal proteins was higher in $Nrf2^{-/-}$ mice than in $Nrf2^{+/+}$ mice. These NRF2-dependent gene products might have key roles in protection against hyperoxic lung injury. Results from our global gene expression profiles provide putative downstream molecular mechanisms of oxygen tissue toxicity.

Keywords: Microarray; Lung; Hyperoxia; Transcription factor; Antioxidant; Free radicals

Reactive oxygen species (ROS) have great potential to damage cellular proteins, lipids, and DNA and have been implicated in various diseases, including atherosclerosis, cancer, neurodegenerative disease, pulmonary fibrosis, and adult respiratory distress syndrome [1]. Oxidative stress results from an imbalance between excess production of ROS and limited cellular antioxidant defense capacity. Recent studies have expanded the known antioxidant defenses to include phase 2 detoxifying enzymes [e.g., NAD(P)H:quinone oxidoreductase 1 (NQO1), glutathione *S*-transferase (GST)], which have antioxidative roles through conversion and secretion of

Abbreviations: ANOVA, analysis of variance; AOX, aldehyde oxidase; ARE, antioxidant response element; CP, 1-Cys peroxiredoxin; DAB, 3,3′-diaminobenzidine tetrahydrochloride; EpRE, electrophilic response element; Ex, carboxylesterase; Gadd45, growth arrest and DNA damage-inducible 45γ; GGT, γ-glutamyl transpeptidase; G6PD, glucose-6-phosphate dehydrogenase; GPx, glutathione peroxidase; GSH, glutathione; GST, glutathione S-transferase; HO-1, heme oxygenase-1; HSP, heat shock protein; MAS5, Microarray Analysis Software 5; MMP, matrix metalloproteinase; NRF2, NF-E2 related factor 2; PKC, protein kinase C; PPARγ, peroxisome proliferator-activated receptor γ; *p*Tyr, phosphorylated tyrosine; QTL, quantitative trait locus; ROS, reactive oxygen species; RT-PCR, reverse transcriptase-polymerase chain reaction; SOD, superoxide dismutase; TXNRD, thioredoxin reductase.

* Corresponding author. Fax: (410) 541 4133.
E-mail address: cho2@niehs.nih.gov (H.-Y. Cho).

0891-5849/$ - see front matter © 2004 Elsevier Inc. All rights reserved.
doi:10.1016/j.freeradbiomed.2004.10.013

harmful oxidized intermediates in malignant cells or tissues [2,3].

Inhalation exposure of laboratory animals to hyperoxia (>95% O_2) has been a useful model to investigate oxidative lung injury due to excess generation of ROS and severe pathology in airways [4,5]. The pathogenesis of oxygen-induced lung injury has been well characterized [6]. However, detailed molecular and mechanistic aspects are not completely understood. Hyperoxia increases expression or activity of many antioxidant enzymes in the lung [e.g., superoxide dismutase (SOD), glutathione peroxidase (GPx), catalase]. Several investigators have demonstrated important protective roles of these antioxidant enzymes in the pathogenesis of oxygen toxicity in laboratory rodents. For example, overexpression of pulmonary *Sod2* in mice provided partial protection against hyperoxic injury [7,8], and targeted deletion of *Sod2* enhanced susceptibility to oxygen [9]. It was also demonstrated that mice deficient in γ-glutamyl transpeptidase (GGT), one of the phase 2 enzymes involved in glutathione (GSH) recycling, had more diffuse lung injury and lower survival rate after hyperoxia exposure, compared to wild-type mice [10,11]. Another potent antioxidant, heme oxygenase-1 (HO-1, HSP32), was protective against oxygen injury in murine lung [12].

We previously identified a significant hyperoxia susceptibility quantitative trait locus (QTL) on chromosome 2 (hyperoxia susceptibility locus 1; *Hsl1*) by genome-wide linkage analysis [13]. This QTL contained a candidate susceptibility gene, *Nrf2*, which encodes the transcription factor NF-E2-related factor 2 (NRF2). Recent investigations have established a critical role for NRF2 in combating oxidative stress generated by ROS, xenobiotics, chemical carcinogens, or other electrophiles in liver [14], lung [15,16], and various cells [17–19]. NRF2 transcriptionally induces antioxidant and defense enzyme genes by binding to the antioxidant response element (ARE) or electrophilic response element (EpRE) as a heterodimer with other transcription factors such as small Maf [15]. We determined that mice with targeted disruption of *Nrf2* had suppressed expression of several ARE-bearing antioxidant/detoxifying enzyme genes and their enzymatic activities after hyperoxia exposure, and these mice were significantly more susceptible to pulmonary oxygen toxicity, relative to wild-type mice [20].

The objective of this study was to identify lung gene expression profiles to understand the molecular mechanisms of oxygen toxicity and NRF2-mediated protection in murine lungs. Using mice with targeted disruption of *Nrf2* ($Nrf2^{-/-}$) and wild-type controls ($Nrf2^{+/+}$), we determined and compared comprehensive gene expression profiles of genes differentially regulated at baseline and in response to oxygen. Results of these studies identified novel pathways through which NRF2 may protect against oxidative tissue injury.

Experimental procedures

Animals

Breeding pairs of ICR/Sv129-$Nrf2^{+/-}$ mice were obtained from a colony at Tsukuba University and maintained in the animal facility at the Johns Hopkins University Bloomberg School of Public Health. $Nrf2^{+/+}$ and $Nrf2^{-/-}$mice were generated following the breeding procedures described previously [14]. Mice were fed a purified AIN-76A diet, and water was provided ad libitum. Cages were placed in laminar flow hoods with high-efficiency particulate-filtered air. Sentinel animals were examined periodically (titers and necropsy) for infection. All experimental protocols conducted in the mice were carried out in accordance with the standards established by the U.S. Animal Welfare Acts, set forth in NIH guidelines and the *Policy and Procedures Manual* (Johns Hopkins University Bloomberg School of Public Health Animal Care and Use Committee).

Oxygen exposure

Mice were placed on a fine mesh wire flooring in a sealed 45-l glass exposure chamber. Food and water were provided *ad libitum*. Sufficient humidified pure oxygen was delivered to the chamber to provide 10 changes/h (7 l/min flow rate). The concentration of oxygen in the exhaust from the chamber was monitored (Beckman OM-11, Irvine, CA, USA) throughout the experiments. The oxygen concentration for all experiments ranged from 95 to 99%. The chambers were opened once a day for <10 min to replace food and water. Male mice (6–8 weeks) of each genotype ($Nrf2^{+/+}$, $Nrf2^{-/-}$) were exposed to either room air or hyperoxia for 24, 48, and 72 h (n = 3/group).

Affymetrix GeneChip array analysis

Total RNA was isolated from the left lung of each mouse using Trizol reagent (Invitrogen, Gaithersburg, MD, USA). Double-stranded cDNA was synthesized from 6 μg of total RNA using the SuperScript Choice system (Invitrogen) with an oligo(dT) primer containing a T7 RNA polymerase promoter (Genset, France). The isolated cDNA was purified by phenol/chloroform extraction and labeled using the ENZO BioArray RNA transcript labeling kit (Enzo Life Sciences, Inc., Farmingdale, NY, USA) to generate biotinylated cRNA. Biotin-labeled cRNA was purified with the Qiagen RNeasy kit (Qiagen, Inc., Valencia, CA, USA) and fragmented randomly to approximately 200 bp (200 mM Tris–acetate, pH 8.2, 500 mM KOAc, 150 mM MgOAc). Each fragmented cRNA sample was hybridized to an Affymetrix Murine Genome U74Av2 oligonucleotide array (Affymetrix, Inc., Santa Clara, CA, USA) for 16 h at 45°C in a GeneChip hybridization oven. Two array chips were used for pooled total RNA from

three mice per exposure group, per time point, per genotype. Microarrays were then washed and stained on the Affymetrix Fluidics Station 400 using instructions and reagents provided by Affymetrix. This involves removal of nonhybridized material and incubation with phycoerythrin–streptavidin to detect bound cRNA (scan 1). The signal intensity was amplified by second staining with biotin-labeled anti-streptavidin antibody, followed by phycoerythrin–streptavidin staining (scan 2). Fluorescent images were read using the Hewlett–Packard G2500A gene array scanner.

Analyses of array data

Each GeneChip underwent a stringent quality control regime. The following parameters were considered: cRNA fold changes (amount of cRNA obtained from starting RNA), scaling factor, percentage of "present" calls, signal intensity, housekeeping genes, internal probe set controls, and visual inspection of the data files for hybridization artifacts. The analysis was performed with Microarray Analysis Software 5 (MAS5) scaling to an average intensity of 800. The expression value (average difference) for each gene was determined by calculating the average of differences in intensity (perfect match intensity minus mismatch intensity) between its probe pairs. The expression analysis files created by MAS5 were transferred to GeneSpring 5.0 (Silicon Genetics, Redwood City, CA, USA) for statistical analyses and characterization of data. Mean intensity of each gene acquired from GeneChip replicates under eight experimental conditions was normalized to that in the air-exposed wild-type ($Nrf2^{+/+}$) group, and these relative ratios were used for all statistical comparison. Array data were analyzed in three ways. First, to determine the effect of NRF2 on basal gene expression, data from air-exposed (control) $Nrf2^{+/+}$ and $Nrf2^{-/-}$ mice were compared by Student's t test. Among significantly ($p < 0.01$) varied genes ($n = 383$), additional restriction identified genes that displayed more than twofold differences in their constitutive expression between genotypes. Second, data from wild-type animals (air, 24, 48, and 72 h) were analyzed by one-way analysis of variance (ANOVA) to determine genes significantly altered by hyperoxia exposure. A p value of 0.05 filtered out 446 genes. Genes increased or decreased more than twofold or 50%, respectively, over the air control at one or more time points were identified and further evaluated. Finally, to identify genes differentially regulated between $Nrf2^{+/+}$ and $Nrf2^{-/-}$ mice during hyperoxia exposure, data from all time points were first restricted by genotype, and then ANOVA filtered out 692 genes with p value of 0.05. Genotype-restricted genes were then further restricted by exposure to find genes ($n = 252$) significantly altered by hyperoxia ($p < 0.05$). The Benjamini and Hochberg False Discovery Rate test was used for the multiple comparisons as necessary. Gene tree applications clustered genes with similar expression pattern, and unique classes of genes with similar kinetics were organized by k-means clustering. Gene ontology procedures were used to evaluate individual genes significantly altered by hyperoxia and significantly varied between $Nrf2^{+/+}$ and $Nrf2^{-/-}$ mice. Venn diagrams isolated common genes that varied basally and by hyperoxia between genotypes.

Total lung RNA isolation for reverse transcriptase-polymerase chain reaction (RT-PCR)

One microgram of total RNA was isolated from right lung homogenates in Trizol (Invitrogen) and was reverse transcribed into cDNA in a volume of 50 μl. PCR amplifications were performed with aliquots of cDNA (5 μl) using a specific primer set for each mouse gene as previously described [20]. Separate, simultaneous PCR for β-actin was done as an internal control, and the volume ratio of each gene cDNA band to β-actin cDNA band was determined using a Bio-Rad Gel Doc 2000 System (Hercules, CA, USA).

Protein isolation and Western blot analyses

Cytoplasmic and nuclear fractions were isolated from right lung homogenates of mice exposed to either air or hyperoxia (48, 72 h) using a Nuclear Extract Kit (Active Motif, Inc., Carlsbad, CA, USA) following the manufacturer's instructions. Cytoplasmic protein (50–100 μg) was separated by sodium dodecyl sulfate–polyacrylamide gel electrophoresis, transferred to nitrocellulose membrane, and immunoblotted with specific primary antibodies for GST-α, GST-μ, and GPx2 (gifts from Dr. C.C. Reddy, Pennsylvania State University) or for glucose-6-phosphate dehydrogenase (G6PD; Novus Biologicals, Inc., Littleton, CO, USA), NQO1 (Novus Biochemicals), phosphorylated protein kinase C-α (*p*PKC-α; Cell Signaling Technology, Inc., Beverly, MA, USA), phosphorylated tyrosine (*p*Tyr; Cell Signaling Technology), collagen type VI (Santa Cruz Biotechnology, Inc., Santa Cruz, CA, USA), HSP70 (Calbiochem Co., San Diego, CA, USA), laminin-B1 (NeoMarkers, Inc., Fremont, CA, USA), and vinculin (Upstate Group, Waltham, MA, USA). Krox-20 (Egr-2, Zfp-25) was detected in nuclear protein (50 μg) using a specific antibody (Covance Research Products, Inc., Richmond, CA, USA). Western blotting was performed two to four times for each protein and representative band images of air and peak expression after hyperoxia are presented.

Lung tissue preparation for immunohistochemistry

Left lung tissues ($n = 2$/group) excised from additional $Nrf2^{+/+}$ or $Nrf2^{-/-}$ mice exposed to hyperoxia (48 or 72 h) or air were inflated gently with zinc formalin, fixed under constant pressure for 30 min, and processed for paraffin embedding. Tissue sections (5 μm thick) were immunologically stained using an affinity-purified rabbit polyclonal anti-

Table 1(A)
Representative genes expressed constitutively higher (≥ twofold) in $Nrf2^{+/+}$ mice than in $Nrf2^{-/-}$ mice

Name	Accession No.	Description
Antioxidant enzymes and related		
Gstb-1	J03952	Glutathione *S*-transferase, μ 1
Gstb-2	J04696	Glutathione *S*-transferase, μ 2
Gstyc	X65021	Glutathione *S*-transferase, Yc
Aox-1	AB017482	Retinal oxidase/aldehyde oxidase
Nrf2	U70475	p45 NF-E2-related factor 2
Cytochrome P450 hydroxylase		
Cyp15a1	M19319	Testosterone 15 α-hydroxylase, 2a4
Cyp2b	M21856	Testosterone phenobarbital inducible type b, 2b10
G-protein-dependent signal transduction		
Gtp1	AJ007972	Interferon-γ-induced GTPase
Grp-R	RU84265	G-protein-coupled, gastrin-releasing peptide receptor
Grp1	AF001871	ARF1 guanine nucleotide exchange factor and integrin binding protein homolog
Gpcr17	D17292	G protein-coupled receptor
Inflammation and immunity		
Cd3-ε	M 23376	CD3 antigen, ε polypeptide, T cell receptor complex
Thy-1, Cd90	M12379	Thymus cell antigen 1, θ
Nkg2d	AF054819	Natural killer costimulating receptor
Tcra	M16118	T cell receptor α chain VJC precursor
Ly112	U18424	Bacterial binding macrophage receptor, MARCO
C1qb	M22531	Complement component 1, q subcomponent, β polypeptide
Ly115	AB023132	Activation-inducible lymphocyte immunomediatory molecule (AILIM)
Mip-1α receptor-like 1	U28405	MIP-1 α chemokine (C-C) receptor 1-like 1
Others		
Tgf β1	AJ009862	Transforming growth factor-β1
Ufo	X63535	AXL receptor tyrosine kinase
Cftr11	X72694	Cystic fibrosis transmembrane conductance regulator
P50, Pol1d2	Z72486	DNA polymerase δ small subunit
Glut-3	M75135	Glucose transporter
Pk-2, Pk-3	X97047	M2-type pyruvate kinase
Epim	D10475	Epimorphin, morphogen
Aq1	L02914	Aquaporin-1

NRF2 antibody raised against a peptide (16 amino acids) mapping at the C-terminus of mouse NRF2 (Covance Research Products, Inc.), an anti-GPx2 antibody, and an anti-collagen VI (α1) antibody (Santa Cruz Biotechnology)

Table 1(B)
Representative genes expressed constitutively higher (≥ twofold) in $Nrf2^{-/-}$ mice than in $Nrf2^{+/+}$ mice

Name	Accession No.	Description
Cell growth and maintenace		
Lop18	J00376	α-A-crystallin, small HSP homology
Hsp68	M12571	68 kDa heat shock protein
Hsp-e71	L40406	Induced by HPV16E7
Ccng	L49507	Cyclin G1
Mtiv	U07808	Metallothionein IV
Fsp, Gro	J04596	Secretory protein KC precursor, GRO1 oncogene
Epidermal-related protein		
Krt-1.13	X03492	47-kDa keratin
Krt-2.4	X03491	57-kDa keratin complex 2, basic
Sprr2a	AJ005559	Small proline-rich protein 2A
Sprr2b	AJ005560	Small proline-rich protein 2B
Sprr3	Y09227	Small proline-rich protein 3
Lgals7	AF038562	Galectin-7, PIG-1, stratified epithelial cell marker
Cx31	X63099	Connexin 31, keratinocyte epidermal connexin
Cytoplasm and extracellular matrix		
Myhs-p	M12289	Myosin, heavy polypeptide 8, skeletal muscle
Myosin light chain 2	M91602	Myosin light chain 2, putative
Myhs-f	AJ002522	Myosin heavy chain 2
Myosin alkali light chain	X12972	Myosin alkali light chain
Pgam2	AF029843	Phosphoglycerate mutase muscle-specific subunit
Tnnt3	L48989	Troponin, skeletal muscle
Fbn-1	L29454	Fibrillin
Dy, Mer	U12147	Laminin-2 α2 chain precursor
Others		
Slpi	AF002719	Secretory leukoprotease inhibitor
Stk	X74736	Receptor tyrosine kinase
Camkii	X14836	Calmodulin-dependent protein kinase IIα
Cox8h	U15541	Cytochrome *c* oxidase subunit VIII-H precursor
Angrp	U22519	Angiogenin-related protein precursor
Ada	M14168	Adenosine deaminase, conversion of adenosine to inosine
Cacng1	AJ006306	Calcium channel, γ-subunit

to localize NRF2, GPx2, and type VI collagen proteins, respectively, using a peroxidase–DAB method. GPx2-stained tissue sections were counterstained with hematoxylin.

Results

Constitutive mRNA expression in $Nrf2^{+/+}$ and $Nrf2^{-/-}$ mice

Three hundred eighty-three genes varied significantly ($p < 0.01$) between $Nrf2^{+/+}$ and $Nrf2^{-/-}$ mice at baseline. Genes ($n = 65$) that were expressed at least twofold more in $Nrf2^{+/+}$ compared to $Nrf2^{-/-}$ mice included those encoding NRF2, antioxidant/phase 2 enzymes, G-protein-linked signal transduction molecules, and T cell receptors (Table 1A). Genes ($n = 82$) that were expressed at least twofold higher in $Nrf2^{-/-}$ compared to $Nrf2^{+/+}$ mice included those encoding heat shock proteins, cytoskeleton/matrix components, and epidermal-related proteins (Table 1B).

Hyperoxia-altered gene expression profiles in $Nrf2^{+/+}$ mice

We demonstrated previously that hyperoxia caused significant lung injury (i.e., inflammation and edema) 72 h after exposure in $Nrf2^{+/+}$ mice; $Nrf2^{-/-}$ mice were significantly more sensitive, with greater lung edema and inflammation after 48 and 72 h exposure compared to $Nrf2^{+/+}$ mice [20]. Pulmonary *Nrf2* mRNA expression was increased immediately after hyperoxia exposure (1.5 h) and its nuclear DNA binding activity enhanced through 72 h in $Nrf2^{+/+}$ mice [13,20]. Based on these findings, we determined time-dependent gene expression profiles before the onset of significant lung injury (24 h) and during the development of severe pathology (48 and 72 h). Hyperoxia significantly ($p < 0.05$) affected expression levels of 446 genes compared to air controls. Genes that were upregulated ($n = 218$) or downregulated ($n = 112$) at 24 h relative to air control levels remained elevated or suppressed, respectively, throughout the exposure (Fig. 1A). Six distinct patterns of gene expression were identified in the lungs of $Nrf2^{+/+}$ mice during hyperoxia (Fig. 1B). Representative genes that were increased ($n = 175$, ≥2-fold) or decreased ($n = 100$, ≥50%) compared to each air control at least once during exposure are listed in Tables 2A and 2B. Sixty-six percent of the 446 genes were upregulated in a time-dependent manner by oxygen (Fig. 1B, sets 1, 2, 3, and 4). These include heat shock proteins, growth factor receptors/ligands, apoptosis proteins, signaling tyrosine phosphatases, extracellular matrix collagens and metalloproteinases, transcription factors/oncogenes, and various enzymes (Table 2A). Genes that were highly induced early (24 h) and remained elevated throughout the exposure included extracellular matrix and cytoskeletal genes (e.g., collagens, laminins, *Mmp-9*, *Vcl*, *Fbn-2*),

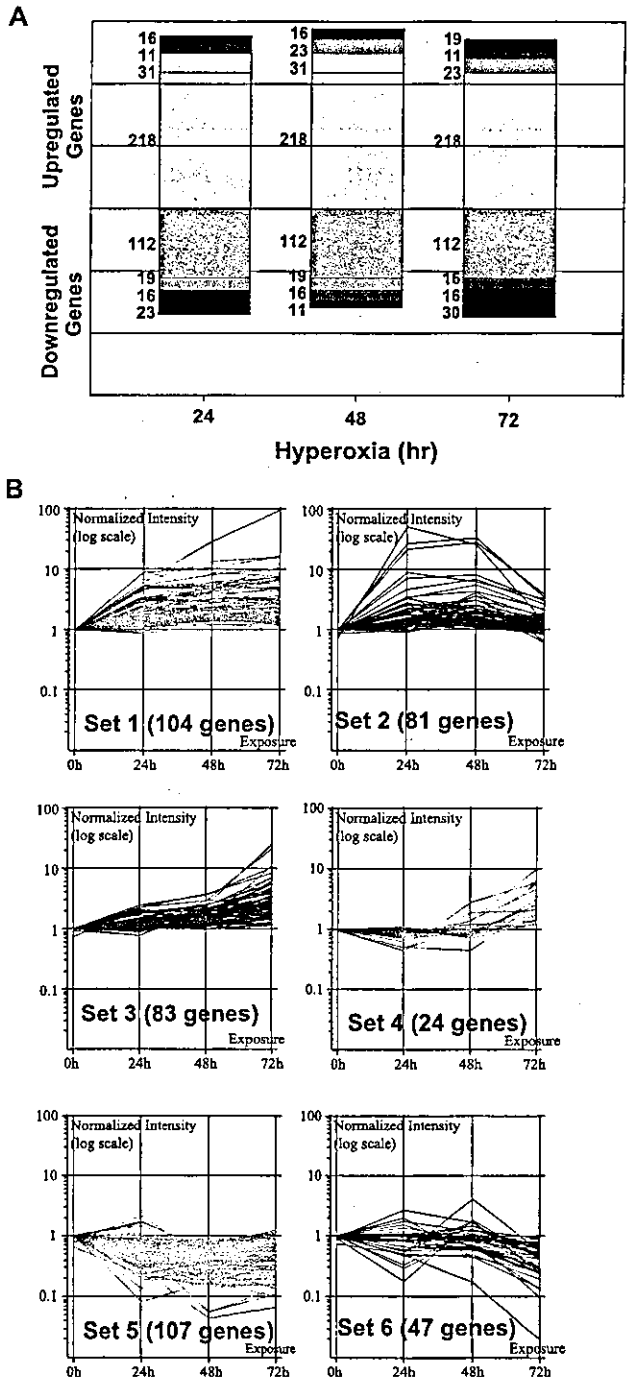

Fig. 1. (A) Number of genes significantly increased or decreased relative to air controls at each time of hyperoxia exposure in $Nrf2^{+/+}$ mice. Matching colors of stacks indicate overlapping genes. (B) Six representative clusters of hyperoxia-induced (sets 1–4) and -suppressed (sets 5 and 6) genes classified based on expression patterns over time course (air and 24, 48, and 72 h O_2). Significantly altered genes ($n = 446$, $p < 0.05$) by hyperoxia in $Nrf2^{+/+}$ mice were evaluated by *k*-means clustering analysis to determine association of gene expression kinetics with gene functions. Expression level of each time point of each gene was normalized by that of air control and expressed as relative log ratio.

inflammation-related genes (e.g., *Ly112*, *Cd104*, *Mic-1*, p-selectin ligand, *Et-1*, cytokine/chemokine/growth factor receptors), transcription factor genes and oncogenes (e.g.,

Table 2 (A)
Representative genes significantly increased (≥ twofold) by hyperoxia in the lungs of wild-type ($Nrf2^{+/+}$) mice

Name	Accession No.	Description	Classification/function	Cluster subset (Fig. 1B)
Cell growth, death, and maintenance				
Hsp68[a]	M12571	68-kDa Heat shock protein	Heat shock response	3
Hsp40	AB028272	Heat shock protein 40	Heat shock response	3
Ho-1, Hsp32	X56824	Heme Oxygenase-1	Heat shock response	2
Nhe-1	L40406	Na^+/H^+ exchanger	Cell pH and volume regulation	1
Mic-1[a]	AJ011967	Macrophage inhibitory compound 1	Growth factor ligand	1
Activin	X69620	Inhibin β-B subunit, TGF receptor ligand	Growth factor ligand	2
Fgfbp1	AF06541	Heparin/fibroblast growth factor binding protein 1	Growth factor ligand	2
Amphiregulin[a]	L41352	EGF family ligand	Growth factor ligand	2
Acvrlk2	L15436	TGF-β type I receptor (Tsk 7L)	Growth factor receptor	1
Mt-2[a]	K02236	Metallothionein II	Metal binding protein, antioxidant	1
Cide-B	AF041377	Cell death activator	Apoptosis	3
Murine A20	U19463	A20 protein	Apoptosis	4
Bax	L22472	Bax α	Apoptosis	2
Gadd45	U00937	Growth arrest and DNA damage-inducible 45γ	DNA repair, cell cycle check point control	2
Signal transduction				
Ptp36	D31842	Protein tyrosine phosphatase	Tyrosine phosphatase	2
Ptprg	L09562	Protein tyrosine phosphatase, receptor type, G1	Tyrosine phosphatase	1
Nttp1[a]	X95518	Neuronal tyrosine threonine phosphatase 1	Tyrosine phosphatase	1
Cd104	L04678	Integrin β4 subunit	Integrin receptor signaling	1
Calcr	U18542	Calcitonin receptor 1b, Ca^{2+}-dependent	Calcium-dependent receptor signaling	2
Mrp8	M83218	Intracellular calcium-binding protein	Calcium-dependent receptor signaling	2
Rhoc	X80638	p21 Rho	Small GTP binding protein	4
Ssecks	AB020886	Src suppressed C kinase substrate	Cytoskeletal signaling	1
Cellular components				
Col1a1	U03419	Procollagen α1 (I)	Extracellular matrix	3
Col4a2	X04647	Collagen α2 (IV)	Extracellular matrix	1
Col6a1	X66405	Collagen α1 (VI)	Extracellular matrix	3
Mmp9	X72795	Gelatinase B	Extracellular matrix	1
Mmp14	AF022432	Zinc endopeptidase	Extracellular matrix	2
Vcl	AI462105	Vinculin cytoskeletal anchoring protein	Cytoskeleton	1
Nf-66[b]	L27220	α internexin, neuronal intermediate filament protein	Cytoskeleton	6
Laman	U87240	Lysosomal α mannosidase	Lysosome	1
Gaa	U49351	Lysosomal α glucosidase	Lysosome	3
Cancer				
Fsp, Gro	J04596	Secretory protein KC precursor, GRO1	Oncogene	2
Rrg	D10837	Lysyl oxidase	Tumor suppressor	1
Ufo[b]	X63535	AXL receptor tyrosine kinase	Oncogene	6
Tx01	Z31362	Gene found in transformed mouse epidermal cell	Cancer related	4
Meca39	U42443	Genetic target for c-Myc regulation	Cancer related	1
Transcription factors				
c-Fos	V00727	Fos cellular oncogene	Transcriptional activator	2
Junc	X12761	Jun oncogene	Transcriptional activator	1
Fra-1[a]	AF017128	Fos-related antigen 1	Transcriptional activator	2
Lrg-21	U19118	Leucine zipper protein	Transcriptional activator	1
Hif1a	AF003695	Hypoxia-inducible factor 1α	Transcriptional activator	2
Sox6[a]	AV246999	EST, similar to Sox (sry-related gene) 6	Transcriptional activator	2
Enzymes				
Pkc-α	M25811	Protein kinase C-α	Kinase	1
Pkch	D90242	nPKC-η	Kinase	2
Hkii	Y11666	Hexokinase II	Kinase	1

Table 2 (A) (*continued*)

Name	Accession No.	Description	Classification/function	Cluster subset (Fig. 1B)
Enzymes				
Cyp15a1	M19319	Testosterone 15 α hydroxylase, 2a4	Cytochrome P450	3
Cyp2b	M21856	Testosterone phenobarbital inducible type b, 2b10	Cytochrome P450	1
Glclc	U85414	γ-Glutamylcysteine synthetase	Glutathione biosynthesis enzyme	2
Gfpt2	AB016780	Glutamine-fructose-6-phosphate amidotransferase 2	Transferase	1
Ggt	U30509	γ-Glutamyl transpeptidase, transmembrane	Transferase	2
Pla2g7	U34277	PAF acetylhydrolase	Hydrolase	2
Spi2/Eb4	M64086	Spi2 proteinase inhibitor	Proteinase inhibitor	2
Mgk-3[b]	X00472	γ-NGF, nerve growth factor, serine protease	Proteinase	5
Mthfd2	J04627	NAD-dependent methylenetetrahydrofolate dehydrogenase	Hydrogenase	2
Inflammation and immunity				
Pai-1	M33960	Plasminogen activator inhibitor		2
Tpa	J03520	Tissue plasminogen activator precursor	Inflammatory peptide	2
Il-6[b]	X54542	Interleukin-6 precursor peptide	Cytokine	4
Fic, Mcp3[a]	X70058	Cytokine	Cytokine	1
Socs-3	U88328	Suppressor of cytokine signaling-3	Cytokine signaling negative regulator	1
Il4r, Cd124	M27960	Interleukin 4 receptor, α	Cytokine receptor	2
G-Csfr	M58288	Granulocyte colony-stimulating factor receptor	Cytokine receptor	1
Ccr1,Mip-1a-r	U29678	MIP-1α/Rantes receptor CCR-1	Chemokine receptor	1
V-1	AJ132098	Vanin 1	Thymic antigen for leukocyte homing	1
Ly112	U18424	Bacterial binding macrophage receptor, MARCO	Macrophage scavenger receptor	1
Others				
Et-1	U35233	Preproendothelin-1	Vasoconstrictor	1
Angl	U72672	Angiogenin-3 precursor	Angiogenesis	3
Dll1	X80903	Delta-like 1	Notch ligand	1

[a] Genes upregulated ≥10-fold at least one time point.
[b] Genes downregulated ≥50% at one time point.

Junc, *Nf-atca*, *Meca39*, *Rrg*), antioxidant enzyme genes (e.g., *Glclc*, *Ggt*), *Pkcα*, and tyrosine phosphatase genes (Fig. 1B, set 1). Early induction of several functionally similar genes (e.g., *Col6a1*, cytochrome P450 hydroxylases/oxidoreductases, *Pkcγ*) as well as heat shock proteins (*Hsp68*, *Hsp40*, *Hsp-e71*) and *Angl* was resolved at 72 h of exposure (Fig. 1B, set 2). Multiple genes with peak induction at 72 h included transcription factors and oncogenes (e.g., *c-Fos*, *Fra-1*, *Gro*), inflammation-related peptides (*Tpa*, *Pai-1*, *Il6*), growth factors and ligands (e.g., *Fgfbp1*, *amphiregulin*), apoptosis (e.g., *Bax*, murine A20), many antioxidant/detoxifying (e.g., *Ggt*, glutaredoxin, *Gstp2*) and other enzymes (e.g., *Pla2g7*, inosine 5′-phosphate dehydrogenase 2, *Mthfd2*), calcium-dependent receptor signaling components (e.g., *Mrp8*, *Calcr*), and transporters (e.g., monocarboxylate transporter 1, calcium-activated chloride channel) (Fig. 1B, sets 3 and 4). Interestingly, some genes such as *Il-6*, *RhoC*, and *Ufo* were more than 50% decreased by hyperoxia during the early time of exposure but were upregulated thereafter (Fig. 1B, set 4). Compared to corresponding baseline expression, the greatest upregulation by hyperoxia was detected for *Mic-1* (90-fold, 72 h), *Angl* (50-fold, 24 h), *Hsp68* (32-fold, 48 h), *amphiregulin* (23-fold, 72 h), and *Fra-1* (20-fold, 72 h).

In contrast, 100 genes were significantly downregulated more than 50% at least once during exposure (Fig. 1B, sets 5 and 6). These genes encode many G-protein-dependent signal transduction elements, cytoskeletal proteins, immunoglobulins, myosin light chain, cardiac actin/troponin, and ESTs (Table 2B).

Genes differentially expressed in $Nrf2^{+/+}$ and $Nrf2^{-/-}$ mice after hyperoxia

ANOVA ($p < 0.05$) restricted by genotype identified 692 genes that were differentially expressed between $Nrf2^{+/+}$ and $Nrf2^{-/-}$ mice during hyperoxia exposure. These genotype-varied genes were then further restricted by exposure and 252 genes whose expression was significantly influenced by hyperoxia ($p < 0.05$) were elucidated. Expression kinetics of these genotype-varied, hyperoxia-

Table 2(B)
Representative genes significantly decreased (≥50%) by hyperoxia in the lungs of wild-type ($Nrf2^{+/+}$) mice

Name	Accession No.	Description	Classification/function
Signal transduction			
Grp-r[c]	RU84265	Gastrin-releasing peptide receptor	G-protein dependent signaling
Gtpi	AJ007972	Interferon induced GTPase	G-protein dependent signaling
Mgbp-2	AJ007970	Murine guanylate binding protein 2	G-protein dependent signaling
Rad	AF084466	Ras-like GTP-binding protein, GTPase	G-protein dependent signaling
Wnt10b	U61970	Secreted factor, protooncogene	Wnt receptor signaling
Cellular components			
Myosin[c]	X12972	Myosin alkali light chain	Cytoskeleton
Mylc2a[c]	AA839903	Myosin regulatory light chain 2	Cytoskeleton
Actc-1	M15501	α-Cardiac actin	Cytoskeleton
Tncc[c]	M29793	Slow/cardiac troponin C	Cytoskeleton
α-actin[c]	M12347	Skeletal α-actin	Cytoskeleton
Tna[c]	X79199	Tetranectin, a plasminogen-binding protein with a C-type lectin domain	Extracellular matrix
Enzymes			
Cpk-m	U55772	p170 Phosphatidylinositol 3-kinase	Kinase
Pgam2[c]	AF029843	Phosphoglycerate mutase, muscle-specific	Mutase
Inflammation and immunity			
Igk-v20	X16678	Ig κ light chain V-region precursor	Ig superfamily member
Igm	M80423	Ig κ chain, putative	Ig superfamily member
Iga[c]	J00475	Ig, secreted form	Ig superfamily member
Car	U90715	Cell surface protein MCAR	Ig superfamily member
Cd3r-ϵ[c]	M 23376	T cell receptor CD3 antigen, ϵ polypeptide	T cell receptor
T3d	X02339	T3 δ-chain	T cell receptor
Bap29	X78684	IgD B-cell receptor-associated protein	B cell receptor
Xlp	AF097632	X-linked lymphoproliferative syndrome gene, SLAM-associated	Immune abnormality
Ifi203	AF022371	Nuclear protein, interferon-inducible protein 203	Nuclear protein
Tnfc	U16985	Lymphotoxin-β	Cytokine
Receptors			
Pgf	D17433	Prostaglandin F receptor	Hormone
Adrb-3	X72862	β-3-Adrenergic receptor	Autonomic nerve
Crbp1	X60367	Cellular retinal binding protein 1	Retinol transport/metabolism
Others			
Wsb1	AF033186	WD-40-repeat protein with a SOCS box	RNA elongation
Gob-4	AB016592	GOB-4 in intestinal goblet cells	Secretion (?)
Ltn-1	M17818	Major urinary protein 1	Urinary
Adipoq	U49915	Adipose tissue-specific glycoprotein	Adipocyte related
ESTs			
AW230066, AW124988, AV347370, AW12534, A690434			

[c] Genes downregulated ≥80% at least one time point.

altered genes was sorted into nine distinct patterns by *k*-means clustering (Fig. 2A), and 175 known genes (i.e., ESTs were excluded) are presented in a gene tree (Fig. 2B). The largest group of genes identified by ontology classification included genes that encode well-known or putative ARE-bearing antioxidant enzymes/redox cycle-related proteins (Table 3A). As shown in a gene tree cluster (Fig. 2D), all of those genes were overexpressed in $Nrf2^{+/+}$ mice relative to $Nrf2^{-/-}$ mice throughout the exposure.

Expression of many genes with no known antioxidant function also varied between $Nrf2^{+/+}$ and $Nrf2^{-/-}$ mice after hyperoxia (Table 3B). For example, genes encoding various enzymes (e.g., *Pkc-α*, *C62*, *Tkt*, *Ldh-2*), cytokine/chemokine receptors, and membrane transporters (e.g., *Pmp34*, *Nkcc1*) were upregulated more in $Nrf2^{+/+}$ mice than in $Nrf2^{-/-}$ mice. Conversely, genes encoding many structural components (e.g., collagens, *Dy*, *Vcl*, *Myh11*) and cell growth/death proteins (e.g., *Tr2l*, *Egr-2*, *Fgfbp1*) were markedly upregulated in $Nrf2^{-/-}$ mice, compared to $Nrf2^{+/+}$ mice.

Hyperoxia decreased genes for G-protein-linked signal proteins, including GTPI (interferon-γ-induced GTPase) and other CNC-basic leucine zipper transcription factors (NFE2, NRF3), significantly more in $Nrf2^{+/+}$ mice, compared to $Nrf2^{-/-}$ mice. In contrast, several chemokine/cytokine genes (e.g., *Mig*, *Mcp-2*, *Angie2*, *Pai-2*), *Wnt-4*, and *Wsb1* were downregulated more in $Nrf2^{-/-}$ mice than in $Nrf2^{+/+}$ mice throughout the exposure.

Overall, the array analyses elucidated several pulmonary antioxidant/detoxifying protein genes (*Aox-1*, *Ex*, *Txnrd1*, *Ftl*, *Cp-2*, *Brp-12*) and non-antioxidant genes, including Tcf3 (transcription factor-3), *Ly112* (bacteria-

binding macrophage receptor, MARCO), *Pkcα*, and *Aq1* (aquaporin-1), that are novel for hyperoxia-induced lung injury. Upregulation of these genes was potentiated in the presence of *Nrf2* during the development of hyperoxic lung injury. Conversely, expression of many collagens (specifically types 1, 4, and 6α), *Vcl*, *Cpx-1*, and *Vanin3* was more highly induced by absence of *Nrf2* in hyperoxic lungs. Venn diagram analysis identified 77 genes that varied significantly at baseline and during hyperoxia exposure ($p < 0.05$) between genotypes (see footnote in Tables 3A and 3B).

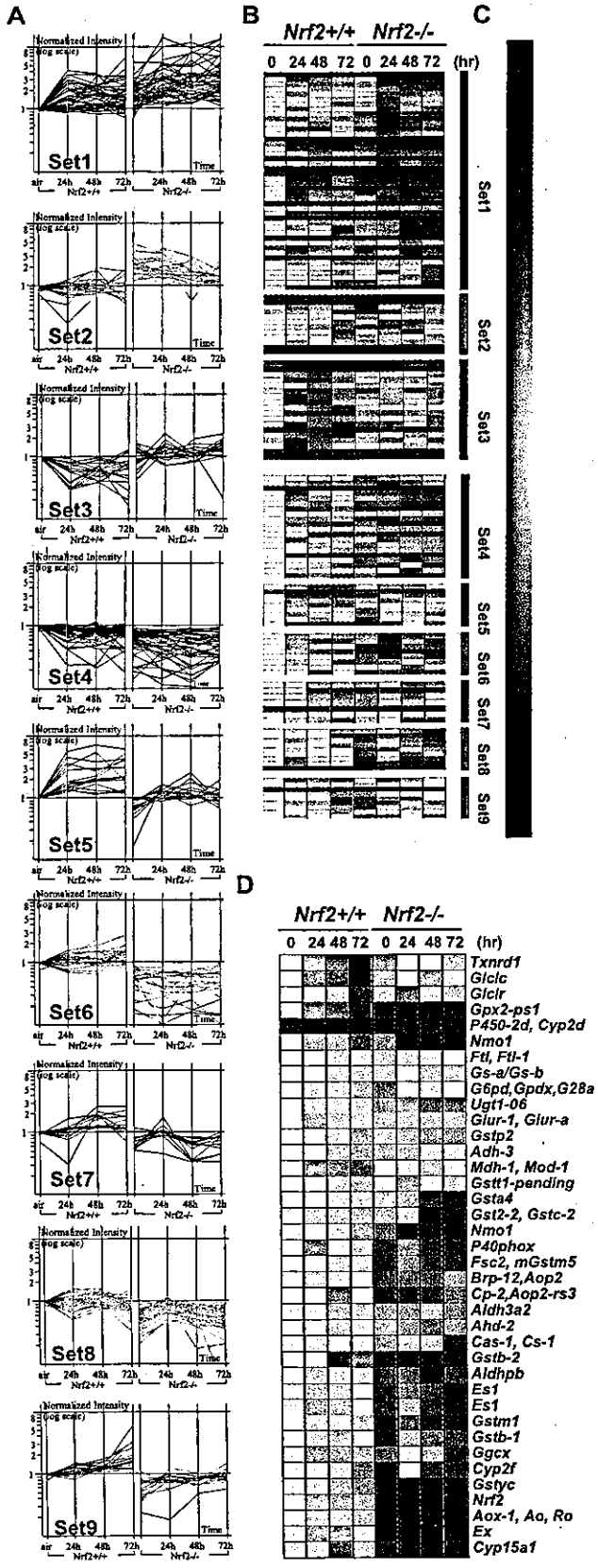

Fig. 2. (A) Nine clusters of hyperoxia-responsive genotype-variable genes (n = 252) between $Nrf2^{+/+}$ and $Nrf2^{-/-}$ mice classified based on expression patterns over time course (air and 24, 48, and 72 h O_2) by k-means clustering analysis. Expression level of each gene was normalized to that of air-exposed $Nrf2^{+/+}$ mice and expressed as relative log ratio. (B) Gene tree clusters of genotype-varied hyperoxia-responsive genes (175 known of 252 genes) in each cluster subset. Color bar beside each cluster matches with graph color of the set in (A). (C) Color bar for expression intensity parameter of gene trees. Yellow color indicates the expression level of standard for normalization, which corresponds to the expression intensity of each gene in normal control (i.e., air-exposed $Nrf2^{+/+}$ mice). Change of color from yellow to red indicates degree of upregulated intensity. Change of color from yellow to blue indicates degree of downregulated intensity. (D) Gene tree cluster of antioxidant/defense enzymes and redox-related protein genes significantly overexpressed in the lungs of $Nrf2^{+/+}$ mice, compared to $Nrf2^{-/-}$ mice. NRF2-regulated antioxidant/defense genes were clustered by gene tree analysis to compare time-dependent changes of gene expression levels by color in two genotypes.

Confirmation of array results by RT-PCR and protein determination by Western blot analyses/ immunohistochemistry

RT-PCR was performed for selected genes that varied markedly between $Nrf2^{+/+}$ and $Nrf2^{-/-}$ mice and confirmed the expression patterns of microarray analysis (Figs. 3 and 4). Protein levels of several genes were detected by Western blot analyses (Fig. 5A). Consistent with their NRF2-dependent mode of gene expression patterns, hyperoxia caused differential protein production of GSTs (α, μ), GPx2, G6PD, NQO1, *p*PKCα, collagen VI, HSP70 (HSP68), Krox-20 (Egr-2, Zfp-25), vinculin, and laminin-B1 in the lung after 48 or 72 h of hyperoxia (peak expressions presented in Fig. 5A). To confirm greater induction of several tyrosine phosphatase genes (e.g., *Ptpb2, C62*) in $Nrf2^{+/+}$ mice than in $Nrf2^{-/-}$ mice, Western analysis was performed with a *p*Tyr antibody. Tyrosine phosphorylation of several proteins (approximate molecular weight 200, 120, 85, 35 kDa) was decreased by hyperoxia in $Nrf2^{+/+}$ mice (Fig. 5A). In contrast, a marked increase of tyrosine phosphorylation was found in many proteins, including ~120-, ~75-, and ~45-kDa proteins, of $Nrf2^{-/-}$ mice after exposure. These proteins were predicted in previous hyperoxia studies [21] as focal adhesion kinase epidermal growth factor receptor, and extracellular signal-regulated kinase.

Immunoperoxide–DAB staining (brown deposition) localized NRF2 prominently in airway epithelium (lining

Table 3 (A)
Antioxidant enzyme and redox cycle-related genes significantly ($p < 0.05$) overexpressed in the hyperoxic lungs of *Nrf2*$^{+/+}$ mice, relative to *Nrf2*$^{-/-}$ mice

Name (cluster subset)	Accession No.	Description	Peak time (h)/ratio[a]
Transferase			
Gstp2 (7)[b,c]	X53451	Glutathione *S*-transferase, π2	72/2.4
Gstyc (4)[c]	X65021	Subunit structure GST YcYc; glutathione transferase	Downregulated/2.8
Gst2-2,Gstc-2 (8)	J03958	Glutathione *S*-transferase, α2 (Yc2)	72/3.9
Gsta4 (8)	L06047	Glutathione transferase, α4, lung-specific	72/4
Gstb-1,Gstb1 (9)[c]	J03952	Glutathione *S*-transferase, μ1	48/2.3
Gstb-2,Gstb2 (4)[c]	J04696	Glutathione *S*-transferase, μ2	Downregulated/2.5
Fsc2,mGstm5 (4)[c]	J03953	Glutathione transferase (EC 2.5.1.18)	Downregulated/1.6
Gstm1 (4)[c]	AI841270	Glutathione *S*-transferase, m1	24/2.1
Gstt1-pending (7)	AI843119	Glutathione *S*-transferase, t1 pending	72/1.8
Ugt1-06 (6)	U16818	UDP glucuronosyl transferase	24/1.7
Oxidoreductase/reductase			
Nmo1 (6)	U12961	NAD(P)H:menadione oxidoreductase	72/36.4
Txnrd1(5)[c]	AB027565	Thioredoxin reductase 1, selenocysteine	72/3.4
Cp-2 (4)	AF093853	1-Cys peroxiredoxin protein 2, CP-2	Downregulated/2.1
Brp-12 (6)	AF093857	1-Cys peroxiredoxin protein, CP-3	24/1.8
Glutathione biosynthesis			
Glclr (9)	U95053	Glutamate-cysteine ligase regulatory subunit	72/3.5
Glclc (5)	U85414	γ-Glutamylcysteine synthetase, gcs heavy chain	72/4.7
Gs-a/Gs-b	U35456	Glutathione synthetase type A1	48–72/1.5
Glur-1,GluR-A (9)	X57497	Glutamate receptor 1	24/1.8
NADPH regenerating enzyme			
G6pd,Gpdx,G28a (9)	Z11911	Glucose-6-phosphate dehydrogenase	72/1.7
Mdh-1,Mod-1 (5)	J02652	Malate NADP oxidoreductase	72/2
Dehydrogenase			
Ahd-2 (4)[c]	M74570	Aldehyde dehydrogenase II	Downregulated/1.3
Aldh3a2 (4)	AV276715	Similar to U14390 aldehyde deydrogenase (Ahd3)	Downregulated/1.4
Aldhpb,Ahd2-like (8)	U96401	Aldehyde dehydrogenase Ahd-2-like	24/2.3
Adh-3 (7)	U20257	Alcohol dehydrogenase, class IV	72/1.9
Esterase			
Es1 (8)	AW226939	Similar to carboxylesterase	24/2.3
Ex (6)	Y12887	Carboxylesterase	24–48/7.9
Ggcx (8)[c]	AI507104	Similar to vitamin-K-dependent γ-carboxylase (human)	24–48/2
Cytochrome P450			
Cyp15a1,D7ucla4 (7)[c]	M19319	Cytochrome P450, 2a4, testosterone 15-α-hydroxylase	48/13.9
Cyp2f (4)[c]	M77497	Cytochrome P-450 naphthalene hydroxylase	Downregulated/3.3
P450-2d,Cyp2d (5)	M27168	Cytochrome P450-16-α-hydroxylase	24–72/2.2
Oxidase			
Gpx2-ps1 (7)	X91864	Gpx2 pseudogene, selenocysteine	72/7.24
Aox-1,Ao,Ro (6)[c]	AB017482	Retinal oxidase/aldehyde oxidase	24–48/5.5
Ftl,Ftl-1 (7)	L39879	Ferritin L-subunit	48–72/1.2
P40phox (4)	U59488	Adaptor protein, phagocyte NADPH-oxidase activator	72/3
Catalase			
Cas-1,Cs-1 (8)	M29394	Catalase 1	24/1.3

[a] *Nrf2*$^{+/+}$:*Nrf2*$^{-/-}$ expression ratio at peak time of expression.
[b] *k*-means clustering subsets in Fig. 2A.
[c] Constitutively overexpressed genes in *Nrf2*$^{+/+}$ mice relative to *Nrf2*$^{-/-}$ mice ($p < 0.05$).

the main stem bronchi, small bronchioles, and terminal bronchioles) as well as in alveolar Type 2 cells and resident macrophages of normal lungs from *Nrf2*$^{+/+}$ mice (Fig. 5B). Hyperoxia induced lung NRF2 deposition time dependently in *Nrf2*$^{+/+}$ mice (72 h shown in Fig. 5B). Higher magnification showed intense localization of NRF2 throughout airway and alveolar epithelia and in nuclei of infiltrated macrophages after hyperoxia (arrows in Fig. 5B). NRF2 was not detected in *Nrf2*$^{-/-}$ mice (only 72 h shown in Fig. 5B). GPx2 (Fig. 5C) and GST-α (data not shown) proteins were predominantly localized in airway/alveolar epithelia and macrophages, where NRF2 was detected, or in smooth muscle cells lining blood vessels. Basal level of GPx2 was higher in *Nrf2*$^{+/+}$ mice, compared to *Nrf2*$^{-/-}$ mice. GPx2 level was highly elevated by hyperoxia in the wild-type mice, whereas marginal increase of GPx2 was detected in *Nrf2*$^{-/-}$mice (Fig. 5A and 5C). Microfibrillar type VI collagen, which plays a role in bridging cells with extracellular matrix, was broadly detected in bronchovascular structures in all control mice. After hyperoxia (72 h shown in Fig. 5D), type VI collagen deposition was enhanced over controls in both strains of mice. However, overall intensity of collagen staining was greater in the susceptible *Nrf2*$^{-/-}$ mice, relative to *Nrf2*$^{+/+}$ mice, with

Table 3 (B)
Representative known genes differentially upregulated by hyperoxia in $Nrf2^{+/+}$ and $Nrf2^{-/-}$ mice

Genes expressed relatively higher in $Nrf2^{+/+}$ mice			Genes expressed relatively higher in $Nrf2^{-/-}$ mice		
Name (cluster)[a]	Accession No.	Description	Name (cluster)[a]	Accession No.	Description
Transcription factor/DNA binding protein			Transcription factor/DNA binding protein		
Nrf2 (6)[b]	U70475	p45 NF-E2-related factor 2	*Egr-2, Krox-20, Zfp-25* (1)	M24377	Zinc finger protein B
Tcf-3 (8)	AJ223069	TCF-3 protein	*Tef-3* (1)	X94441	Transcription factor
Lim1 (9)	Z27410	Putative transcription regulator	*Lrg-21* (1)	U19118	Leucine zipper protein
			Orf1 (1)	AB019029	Cofactor required for Sp1 transcriptional activation subunit 2
			Zfp144 (1)	D90085	ORF for Mel-18
			N10 (2)	X16995	Nuclear protein, hormone receptor, zinc finger protein
Cell death/growth/maintenance			Cell death/growth/maintenance		
Fgfbp1 (9)	AF065441	FGF binding protein 1	*Rirl1, Tr2l* (1)	U70210	Similar to the C-terminus of rat transcriptional activator FE65
Fgrp, Fr-1 (9)	U04204	Aldose reductase-related protein	*Tsg6* (1)	U83903	TNF-stimulated gene 6, TNF-receptor ligand
Nr1c3, Ppar-γ (6)[b]	U10374	Peroxisome proliferator-activated receptor γ	*Tgf-β2* (1)	X57413	Transforming growth factor-β 2 precursor
Cdh15 (7)	AJ245402	Cadherin, cell adhesion molecule	*Wisp1* (1)	AF100777	Connective tissue growth factor-related protein
β Ig-h3 (5)	L19932	P68 Ig-type growth factor, cell adhesion inhibitor	*Flk-1* (1)	X70842	FLK endothelial cell growth factor
Nl (9)	M14220	Neuroleukin, lymphokine, growth factor	*Aigf, Fgf-8* (1)	D12483	Fibroblast growth factor
			Hsp68 (1)[c]	M12571	68-kDa heat shock protein
			Extracellular matrix/cytoskeleton		
			Col1a1 (1)	U03419	Procollagen α 1 (I)
			Col6a-2 (1)	Z18272	Collagen α 2 (VI)
			Col18a1 (1)[c]	L22545	Collagen α 1 (XVIII)
			Col13a1 (1)[c]	U30292	Collagen α 1 (XIII)
			Dy, Mer, Merosin (1)[c]	U12147	Laminin-2 m-chain; merosin α2 chain; merosin m-chain
			Lamb-1 (1)[c]	X05212	Laminin B1
			Eln (1)	U08210	Tropoelastin
			Smsmo (1)	AJ010305	Smoothelin L1, large isoform
			Fbln1 (1)	X70853	BM-90/fibulin
			Fbln2 (1)[c]	X75285	Fibulin-2
			Vcl (1)	L18880	Vinculin
			Actvs (3)	X13297	Actin, α2, smooth muscle, aorta
			Act-4, Acta3 (1)	U20365	Smooth muscle γ-actin
			Fbn-1 (1)[c]	L29454	Fibrillin
			Myh11 (1)	D85923	Myosin heavy chain 11, smooth muscle
Signal transduction			Signal transduction		
Strap (6)	AF096285	TGF-β receptor-associated protein	*Chrm-4, M4* (3)	X63473	m4 muscarinic acetylcholine receptor
Bet, Ptpb2 (9)	D83203	Receptor-type protein tyrosine phosphatase	*Achr-2, Acrb* (3)	M14537	Acetylcholine receptor β subunit

(continued on next page)

Table 3 (B) (*continued*)

Genes expressed relatively higher in *Nrf2*$^{+/+}$ mice			Genes expressed relatively higher in *Nrf2*$^{-/-}$ mice		
Name (cluster)[a]	Accession No.	Description	Name (cluster)[a]	Accession No.	Description
Gp1bb (6)	AB001419	Platelet glycoprotein 1b β, PDGF ligand	*Npyr* (2)	Z18280	Neuropeptide hormone receptor NPY-1
Ptp36 (5)	D31842	Protein tyrosine phosphatase	*Fnra* (1)	X79003	Integrin α5 subunit
			Scn71, Nav2.3, Nag (2)	L36179	Voltage-gated sodium channel protein
Transport			Transport		
Nkcc1, Mbsc2 (9)	U13174	Putative basolateral Na-K-2Cl cotransporter	*Cat2* (1)	L03290	Cationic amino acid transporter-2
Nramp (7)	L13732	Integral membrane protein, candidate for Bcg gene	*Pmp34* (2)	AJ006341	Peroxisomal integral membrane protein PMP34
Slc6a6 (4)	AI042802	Similar to Na- and Cl-dependent taurine transporter			
Twik-1 (9)	AF033017	TWIK-1 K^+ channel			
Cd71 (8)	X57349	Transferrin receptor			
Enzymes			Enzymes		
Pkc-α (5)	M25811	Protein kinase Cα	*His, Hsd, Histidase* (1)	L07645	Histidine ammonia-lyase
Tkt, P68 (5)	U05809	Transketolase	*Cpx-1* (1)	AF077738	Metallocarboxypeptidase, similar to CPX-2 and AEBP1
Ldh-2, Ldhb (8)	X51905	Lactate dehydrogenase 2, B chain	*Ly-41, Npps, Pca, Npp1* (1)	J02700	Plasma membrane glycoprotein, ecto-nucleotide phoaphatase
Er-udpase (6)	AJ238636	Nucleoside diphosphatase	*Cf7, FvII* (1)	U66079	Coagulation factor VII, coenzyme A
Pmm2 (6)	AF043514	Phosphomannomutase, SEC53 homolog	*Cpk-m* (1)	U55772	P170 phosphatidyl inositol 3-kinase
Macr1 (6)	U89906	α-Methylacyl-CoA racemase	*Calnc* (3)	M81475	Phosphoprotein phosphatase, calmodulin-dependent
mCask (8)	Y17138	mCASK-B	*C5d* (3)	AB016248	Sterol-C5-desaturase
C62 (8)[b]	U96724	Putative phosphoinositide 5-phosphatase type II			
Dbt (9)	L42996	α-Ketoacid dehydrogenase, mitochondrial			
Pla2g7 (7)	U34277	PAF acetyl hydrolase			
Inflammation and immunity			Inflammation and immunity		
Cathepsin s (9)[b]	AJ223208	Cysteine protease, antigen presentation	*RegIIIγ* (1)	96064	Regenerating gene in islet β-cells, mitogenic
Ly112 (5)[b]	U18424	Bacteria binding macrophage receptor, MARCO	*C10* (1)[c]	M58004	Small inducible cytokine A6
Ccr1,Mip-1a-r (5)	U29678	MIP1-α/Rantes receptor, G-protein coupled	*Vanin 3* (1)	AJ132103	Vanin-3, leukocyte adhesion and homing
Ngp (5)	L37297	Myeloid secondary granule protein	*Scya11* (3)	U77462	Eotaxin, C-C chemokine family
			Evi-1 (3)	M21829	Ecotropic viral integration site1, transcription regulator
			Ltf (1)	J03298	Lactotransferrin precursor, estrogen inducible protein
			Igk-v28 (3)	Z70661	Single chain antibody ScFv
Others			Others		
Aq1 (5)[b]	L02914	Aquaporin-1	*Cx31* (1)[c]	X63099	Connexin 31, gap juction protein
Endomucin (8)[b]	AB034693	Endomucin-1, sialomucin	*Msemk1* (1)	AB017532	msemk1p

Table 3 (B) (*continued*)

Genes expressed relatively higher in $Nrf2^{+/+}$ mice			Genes expressed relatively higher in $Nrf2^{-/-}$ mice		
Name (cluster)[a]	Accession No.	Description	Name (cluster)[a]	Accession No.	Description
Mcl (7)[b]	AF061272	Macrophage-restricted C-type lectin	*Alox12l, 12-Lo* (3)	L34570	12-Lipoxygenase
Creg (9)	AF084524	Cellular repressor of E1A-stimulated gene	*Anx6, Cabm* (2)	X13460	Lipocortin
Phll1 (5)	AB000777	Photolyase/blue-right receptor homolog			

[a] *k*-means clustering subsets in Fig. 2A.
[b] Constitutively overexpressed genes in $Nrf2^{+/+}$ mice relative to $Nrf2^{-/-}$ mice ($p < 0.05$).
[c] Constitutively overexpressed genes in $Nrf2^{-/-}$ mice relative to $Nrf2^{+/+}$ mice ($p < 0.05$).

distinct localization in bronchial basement membrane, endothelium, and alveolar septum.

Discussion

We previously determined NRF2-dependent pulmonary antioxidant/defense enzymes that are potentially important in the protection against pulmonary oxygen toxicity [20]. The present study identified novel genes responsive to oxidative stress and expanded the number of NRF2-regulated genes that could engage, directly or indirectly, in the pathogenesis of oxidative pulmonary injury and protection.

The largest cluster of genes with greater basal and hyperoxia-induced expression in $Nrf2^{+/+}$ mice compared to $Nrf2^{-/-}$ mice contained more than 38 antioxidant/detoxifying enzyme and redox cycle-related protein genes (see Table 3A and Fig. 2D). One of these, thioredoxin reductase (TXNRD), maintains a high ratio of reduced to oxidized thioredoxin, a primary intracellular thiol with redox-buffering capacity similar to that of GSH to reduce H_2O_2 and lipid peroxides [22]. One-Cys peroxiredoxin (CP) belongs to a family of recently recognized antioxidants and is abundant in the lung. CP has GPx and phospholipase A2 activity to protect against lung oxidant injury and phospholipid metabolism [23]. Identification of these antioxidant genes as well as multiple GST isozyme genes, *Glclc*, *Glclr*, *Gpx2*, *Gs-a, Gs-b,* and *G6pd,* suggests that a substantial portion of NRF2-mediated pulmonary protection against hyperoxic injury is via cellular defense enzymes associated with thiol metabolism and homeostasis pathways, as depicted in Fig. 6A. Recently, a protective role for a phase 2 defense enzyme (GGT) was functionally determined in hyperoxia models [10,11], which supports the critical antioxidative role of a NRF2–thiol mechanism in oxidative tissue damage. Importantly, we localized NRF2 in the mouse lung. These novel findings indicate that NRF2 is found in airway epithelium and macrophages, where antioxidant enzymes (e.g., GPx2, GSTs) are predominantly expressed. It also further supports functional association of NRF2 and thiol-related antioxidants in protection of the lung from oxidative insult.

Additional NRF2-dependent putative antioxidants in hyperoxic lungs included carboxylesterase (Ex), aldehyde oxidase (AOX)-1, aldehyde dehydrogenases (AHD-2, ALDH3a2, ALDHpb), and ferritin (L subunit). Each has demonstrated antioxidative or detoxifying activity that protects tissues from oxidative stress or injury by various xenobiotics [24–29]. These genes were also recently found to be NRF2-dependent in array analyses with liver models of chemical carcinogenesis [30,31]. Among them, ferritin has a potentially important antioxidant role by sequestering iron to limit its participation in ROS formation, and Tsuji et al. [27] recently identified ARE in the promoter of the ferritin heavy chain. Evidence exists that ferritin protects against hyperoxic lung injury [28] and cellular oxidative stress against xenobiotics [24]. Results of the present study also elucidated several NRF2-dependent cytochrome P450 hydroxylases containing an ARE-like motif (xenobiotic response element) for their transcriptional activation [24]. We found NRF2-dependent non-P450 oxidative enzymes such as alcohol dehydrogenase (ADH-3), AOX-1, and several aldehyde dehydrogenases, some of which bear an ARE motif in their promoters [26].

Novel NRF2-dependent genes upregulated by hyperoxia, but not involved with antioxidant defense, included *Pkc*-α, the major pulmonary PKC isozyme. A protective role for PKC in airways was demonstrated by a genetic linkage analysis in which *Pkc*-α was identified as a candidate protective gene in asthma and pulmonary adenocarcinoma [32]. Importantly, PKC is known to act on the upstream signaling pathway of NRF2 to facilitate its translocation into nuclei. Huang et al. [33] first proposed phosphorylational activation of NRF2 (at Ser40) by PKC. They demonstrated that the Ser40Ala mutation in *Nrf2* led to failure of NRF2 to dissociate from Keap1, a cytosolic inhibitor of NRF2, and inhibited its translocation in response to oxidative stress. This concept has been confirmed by other investigations [34]. Hyperoxia-induced GPx gene expression was dependent on activated PKC in cultured endothelial cells [35]. It is therefore postulated that activation of PKC by hyperoxia induces GPx probably through NRF2 transactivation.

Kinetics of potentially important genes responsive to hyperoxic stress were determined in wild-type ($Nrf2^{+/+}$)

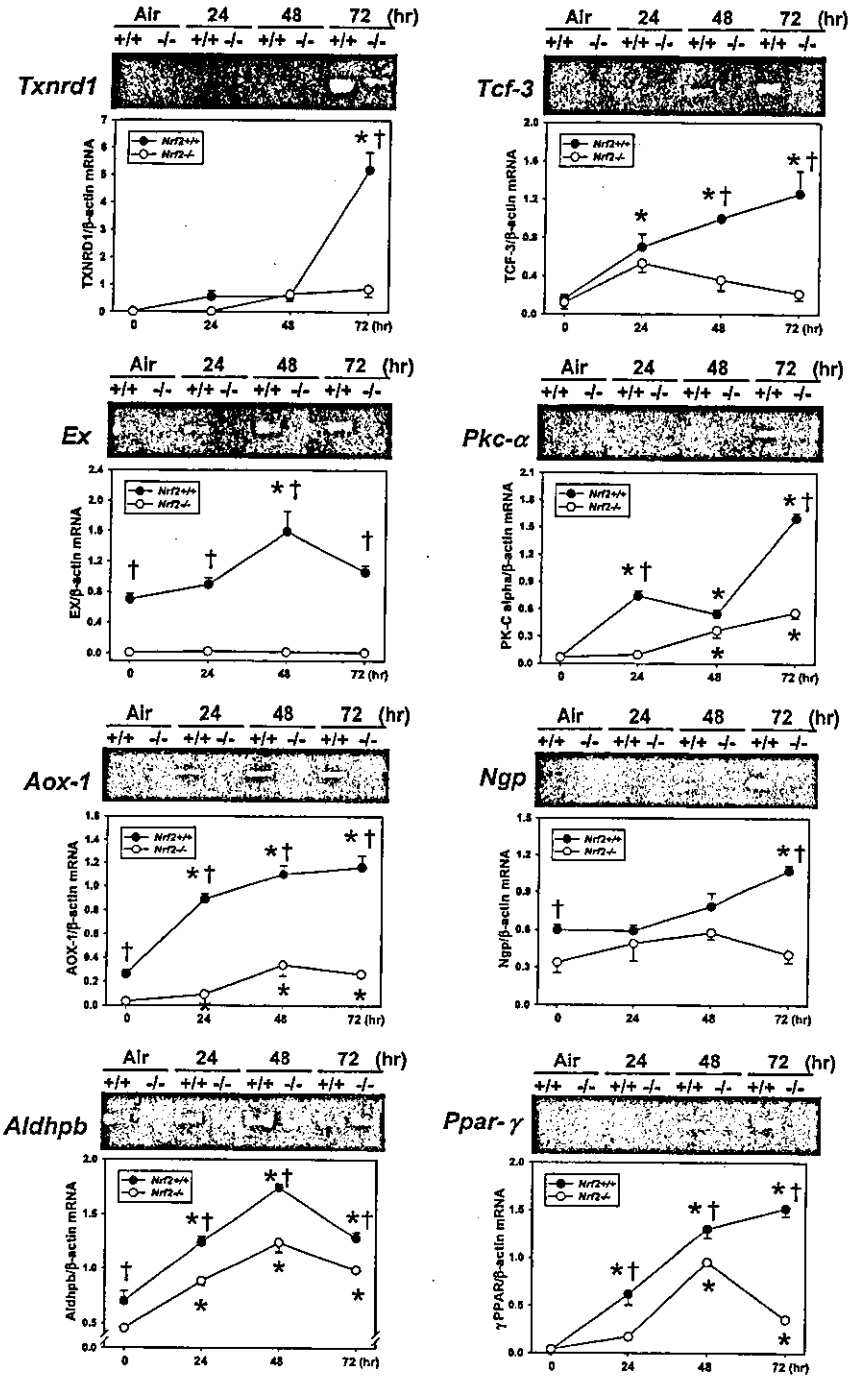

Fig. 3. RT-PCR analyses of representative genes expressed higher in $Nrf2^{+/+}$ mice than in $Nrf2^{-/-}$ mice after hyperoxia exposure. Total lung RNA isolated from the right lung of each mouse (left lung of which was used for array analysis) was processed for RT-PCR analysis to confirm microarray results. Digitized images of cDNA bands on agarose gels were quantitated and normalized to an internal control gene (β-actin) cDNA band. All data are represented as the group means ± SEM (n = 3/group). * Significantly different from genotype-matched air control ($p < 0.05$). †, Significantly different from time-matched $Nrf2^{-/-}$ mice ($p < 0.05$). Representative gel image of each gene is shown above each graph.

animals (see Tables 2A and 2B), and many of the significantly altered genes have not been previously investigated in hyperoxia models. Hyperoxia markedly upregulated numerous genes as early as 24 h before the onset of significant morphological and biological signs of injury (i.e., pulmonary edema, inflammation, septal hyperplasia), and their elevated expression persisted through 48 h or 72 h. Recently, Perkowski et al. [36] determined hyperoxia-responsive genes in the lungs of female C57BL/6J mice at 8–48 h using a Clontech microarray platform. Categories of common genes induced by hyperoxia in their study and the current gene expression profiles of $Nrf2^{+/+}$ mice included genes that encode antioxidants (e.g., GSTs, GPx, HO-1),

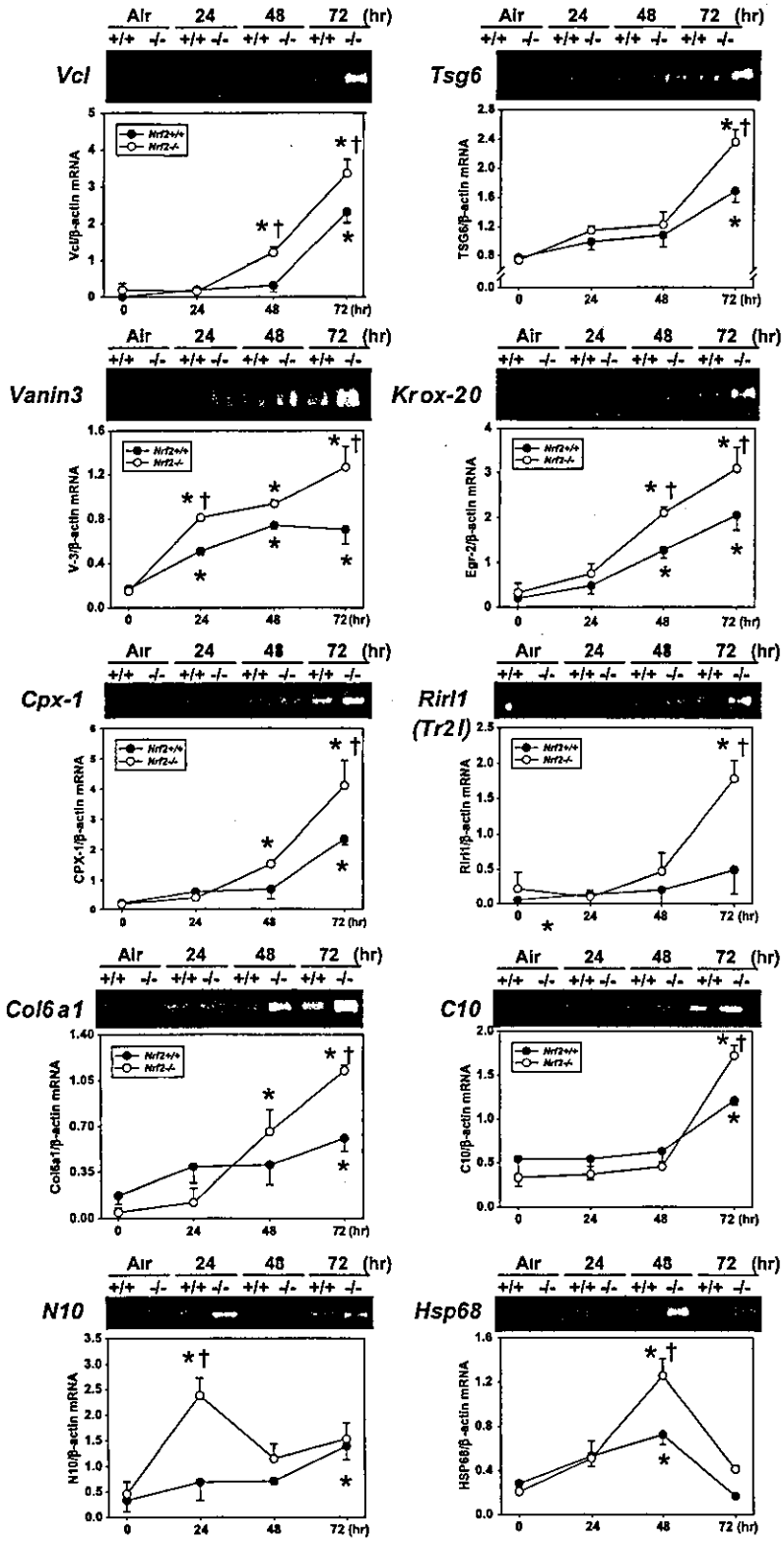

Fig. 4. RT-PCR analyses of representative genes expressed higher in $Nrf2^{-/-}$ mice than in $Nrf2^{+/+}$ mice after hyperoxia exposure. Total lung RNA isolated from the right lung of each mouse, (left lung of which was used for array analysis) was processed for RT-PCR analysis to confirm microarray results. Digitized images of cDNA bands on agarose gels were quantitated and normalized to an internal control gene (β-actin) cDNA band. All data are represented as the group means ± SEM ($n = 3$/group). * Significantly different from genotype-matched air control ($p < 0.05$). † Significantly different from time-matched $Nrf2^{-/-}$ mice ($p < 0.05$). Representative gel image of each gene is shown above each graph.

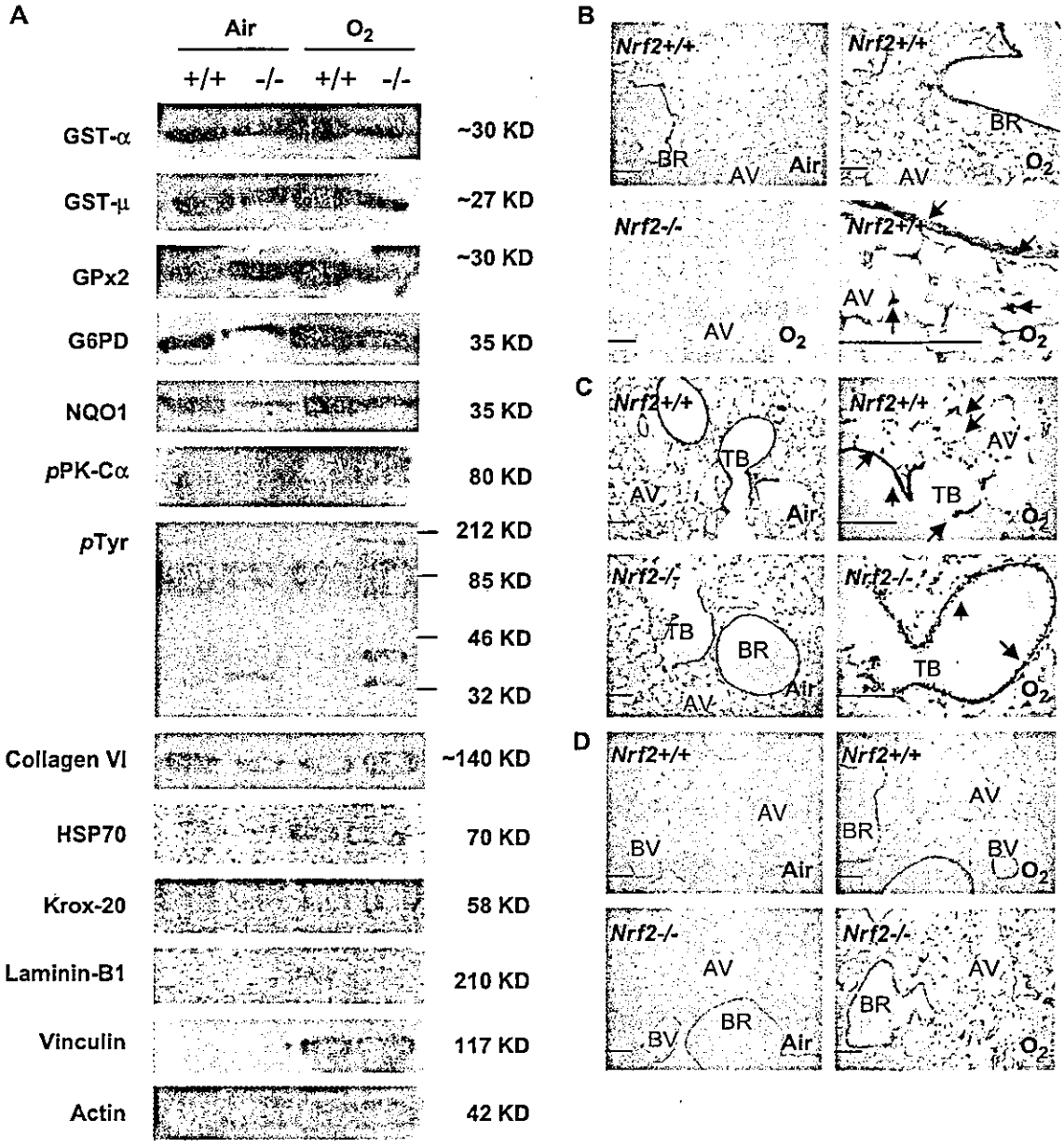

Fig. 5. (A) Differential protein levels of NRF2-dependent genes determined by Western blot analyses. Cytoplasmic and nuclear protein was isolated from right lung homogenates of $Nrf2^{+/+}$ and $Nrf2^{-/-}$ mice exposed to either air or hyperoxia (48 and 72 h), and aliquots were subjected to Western blot analyses using specific antibodies for glutathione *S*-transferase (GST)-α and -μ, glutathione peroxidase(GPx) 2, glucose-6-phosphate dehydrogenase (G6PD), NADP(H):quinone oxidoreductase (NQO) 1, phosphorylated protein kinase C (*p*PKC) α, phosphorylated tyrosine (*p*Tyr), type VI collagen (α1), heat shock protein (HSP) 70, Krox-20 (Egr-2, Zfp-25), laminin-B1, and vinculin. Actin was determined as a constitutive protein control. Representative images from two to four independent analyses of air and peak expression are shown. (B–D) Lung tissue sections were immunohistochemically stained to localize NRF2 [(B) Note high magnification of $Nrf2^{+/+}$ lung section exposed to hyperoxia. Only hyperoxia-exposed lung section presented for $Nrf2^{-/-}$ mice], GPx2 (C), and collagen VI (D) in the lungs from $Nrf2^{+/+}$ and $Nrf2^{-/-}$ mice after air and hyperoxia exposure (72-h data shown). Brown staining indicates antigen deposition. AV, alveoli; BR, bronchiole; TB, terminal bronchiole; BV, blood vessel. Bars indicate 100 μm.

metallothionein, apoptosis genes such as *Bax*, calcium channel genes, and genes related to vascular endothelium. These investigators analyzed data focused on early events (at 24 h) such as apoptosis because hyperoxia-modulated genes were significantly changed mostly at 24 h after hyperoxia in their study. They also demonstrated that more genes were downregulated rather than upregulated at this early time of exposure in these mice. Differences in genes on the array chips or in animals (gender or strain) may account for differences between studies.

Another distinctive gene cluster induced by hyperoxia included extracellular matrix proteins (see Table 2A). In addition to collagens, excessive deposition of microfilaments such as laminins and fibrillins has been considered as an important marker of epithelium-to-mesenchyme

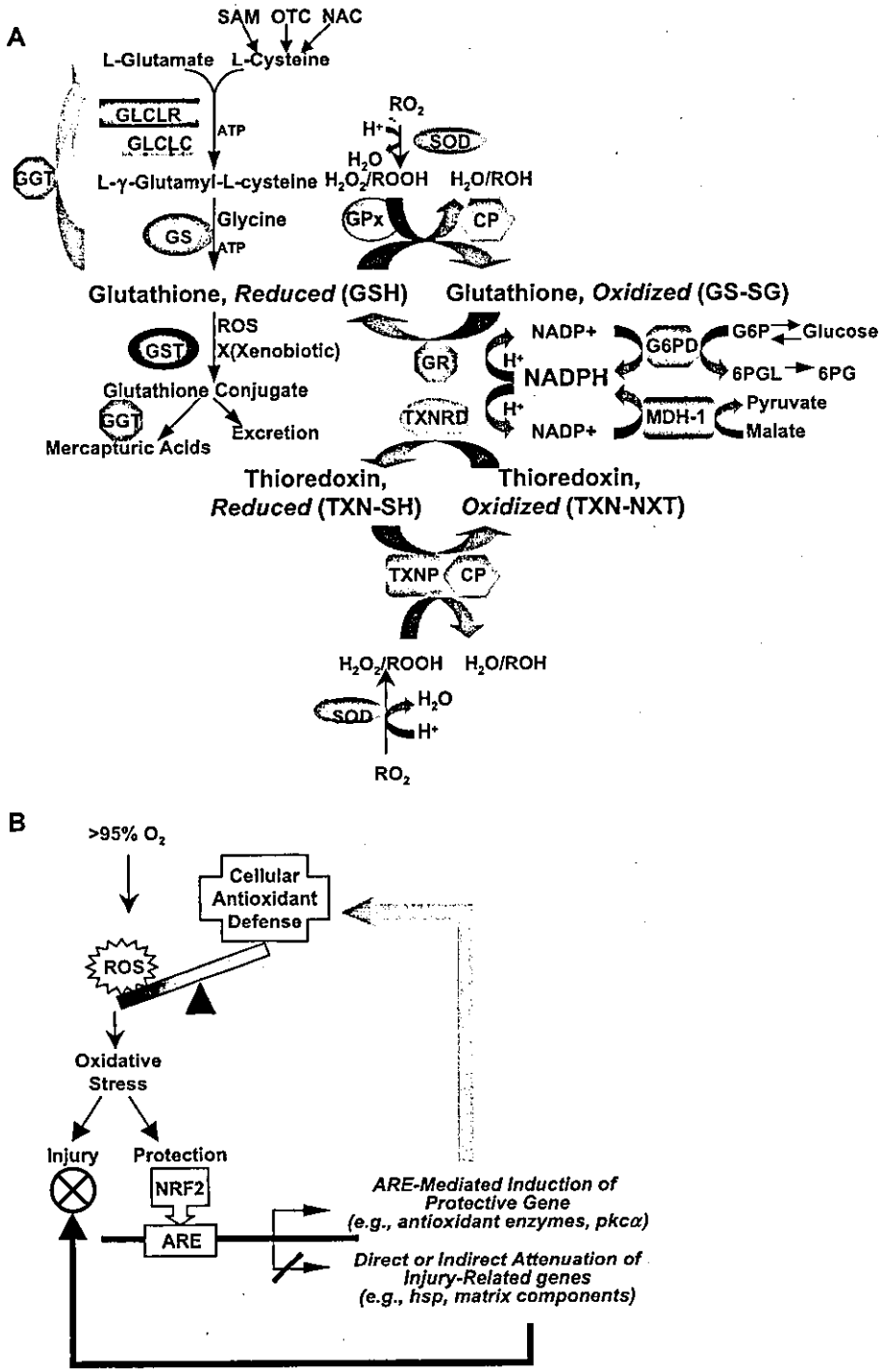

Fig. 6. (A) Proposed primary downstream pathway of NRF2 presents the role of ARE-containing thiol-related antioxidant/redox-cycle enzymes in hyperoxia-injured lungs. SOD, superoxide dismutase; GLCLR, γ-glutamylcysteine ligase regulatory subunit; GLCLC, γ-glutamylcysteine ligase catalytic subunit; GS, glutathione synthetase; GPx, glutathione peroxidase; GR, glutathione reductase; CP, 1-cysteine peroxiredoxin; GST, glutathione *S*-transferase; TXNRD, thioredoxin reductase; TXNP, thioredoxin peroxidase; G6PD, glucose-6-phosphate dehydrogenase; MDH-1, malate dehydrogenase-1; GGT, γ-glutamyl transpeptidase; SAM, *S*-adenosyl-L-methionine; NAC, *N*-acetyl-L-cysteine; OTC, 2-oxothiazolidine-4-carboxylate; 6PGL, 6-phosphogluconolactone; 6PG, 6-phosphogluconate. (B) Putative simplified scheme of hyperoxic injury and protective role of NRF2 in lungs.

transition during airway remodeling [37]. Vinculin, an actin-binding adhesion molecule for cytoskeletal anchoring to the nuclear and cell membrane, is known to increase during the change of cytoskeletal architecture by oxidative stress [38]. Proteolytic activity of various matrix metalloproteinases (MMPs) including MMP9 produced by resident lung cells and various inflammatory cells is also important in pulmonary reepithelialization immediately after acute inhalation injury [39,40]. In addition, the plasminogen system (i.e., plasminogen, urokinase-type

plasminogen activator, tissue-type plasminogen activator in matrix is the primary physiological fibrinolytic pathway through MMP activation [41]. Taken together, marked induction of these genes in the injured lung strongly indicates their coordinated roles in the airway repair and remodeling process after hyperoxia exposure. Importantly, many of these extracellular matrix and cytoskeletal genes were more highly expressed in susceptible $Nrf2^{-/-}$ mice compared to $Nrf2^{+/+}$ mice after exposure (see Table 3B). Some genes were also constitutively higher in $Nrf2^{-/-}$ mice. This suggests that NRF2 is involved in their transcriptional regulation in either normal or oxygen-injured lungs. No evidence exists for the presence of ARE sequences in their promoter. It is therefore postulated that instead of direct modulation of these genes by NRF2, increased oxidative burden by suppression of antioxidant defense mechanisms in $Nrf2^{-/-}$ mice secondarily triggers matrix and structural component genes required for adaptation responses (i.e., repair or reconstitution) against further lung injury (Fig. 6B).

It is well known that hyperoxia causes DNA injury and apoptosis in pulmonary tissues. Many genes involved in apoptosis/survival signals were identified to be hyperoxia inducible in the present analysis (see Table 2A). Among these is *Gadd45* (growth arrest and DNA damage-inducible 45γ), which is regulated through p53 in hyperoxia-injured lungs [42] as well as in many types of cancer cells, including those in the lung [43], to repair DNA fragmentation. Genes encoding heat shock response proteins comprise another cluster that is highly induced by hyperoxia at the early phase of injury. Similar to the extracellular matrix components, early induction of 70-kDa HSP genes (*Hsp68* and *Hsp40*, [44]) was potentiated in the absence of *Nrf2*. This suggests their participation in lung stress responses against hyperoxia as previously indicated [45].

Although our current study focused on genes upregulated by inhaled oxygen, numerous genes and ESTs were downregulated throughout exposure (see Table 2B). Genes such as GTPases, including *Gtpi* (interferon -γ-induced GTPase) may be particularly important because they were differentially suppressed between $Nrf2^{+/+}$ and $Nrf2^{-/-}$ mice. GTP-binding/hydrolyzing proteins induced cell proliferation and hypertrophy via activation of downstream mitogen-activated protein kinase pathways in fibroblasts and endothelial cells after ROS or hyperoxia exposure [22]. *Gtpi* has been shown to induce proliferation of lung cells [46]. Further investigation will be necessary to understand the roles of these downregulated genes in oxidative injury models.

In summary, microarray analysis determined kinetics of hyperoxia-responsive pulmonary genes and identified potentially important NRF2-regulated genes. Newly identified pulmonary antioxidant enzyme/redox-related proteins (e.g., TXNRD1, Ex, CP-2) as well as novel non-antioxidant proteins (e.g., PKC-α, TCF-3, PPARγ) might have key roles in the NRF2-mediated protection against hyperoxic lung injury. Extracellular matrix and structural components as well as heat shock proteins may also have a central role in oxygen-induced airway injury and repair mechanisms. Results from this study provide important insight into molecular mechanisms underlying oxidative lung injury.

Acknowledgments

The National Institute of Environmental Health Sciences, National Institutes of Health, Department of Health and Human Services, and grants (to S.R.) from the National Institutes of Health (ES-03819, ES-09606, HL-073996, HL-66109, HL-57142, NHLBI U01 HL-66614-01, and CA-44530) supported this research. The authors thank Tomohiro Oshimura for his help with the array analyses.

References

[1] Halliwell, B.; Gutteridge, J. M.; Cross, C. E. Free radicals, antioxidants, and human disease: where are we now? *J. Lab. Clin. Med.* 119:598–620; 1992.

[2] Fahey, J. W.; Talalay, P. Extracellular superoxide dismutase in the airways of transgenic mice reduces inflammation and attenuates lung toxicity following hyperoxia. *Food Chem. Toxicol.* 37:973–979; 1999.

[3] Itoh, K.; Ishii, T.; Wakabayashi, N.; Yamamoto, M. Regulatory mechanisms of cellular response to oxidative stress. *Free Radic. Res.* 31:319–324; 1999.

[4] Clerch, L. B. Post-transcriptional regulation of lung antioxidant enzyme gene expression. *Ann. N. Y. Acad. Sci.* 899:103–111; 2000.

[5] Ho, Y. S.; Dey, M. S.; Crapo, J. D. Antioxidant enzyme expression in rat lungs during hyperoxia. *Am. J. Physiol.* 270(5 Pt 1):L810–818; 1996.

[6] Crapo, J. D. Morphologic changes in pulmonary oxygen toxicity. *Annu. Rev. Physiol.* 48:721–731; 1986.

[7] Folz, R. J.; Abushamaa, A. M.; Suliman, H. B. Extracellular superoxide dismutase in the airways of transgenic mice reduces inflammation and attenuates lung toxicity following hyperoxia. *J. Clin. Invest.* 103:1055–1066; 1999.

[8] Ho, Y. S.; Vincent, R.; Dey, M. S.; Slot, J. W.; Crapo, J. D. Transgenic models for the study of lung antioxidant defense: enhanced manganese-containing superoxide dismutase activity gives partial protection to B6C3 hybrid mice exposed to hyperoxia. *Am. J. Respir. Cell Mol. Biol.* 18:538–547; 1998.

[9] Tsan, M. F.; White, J. E.; Caska, B.; Epstein, C. J.; Lee, C. Y. Susceptibility of heterozygous MnSOD gene-knockout mice to oxygen toxicity. *Am. J. Respir. Cell Mol. Biol.* 19:114–120; 1998.

[10] Barrios, R.; Shi, Z. Z.; Kala, S. V.; Wiseman, A. L.; Welty, S. E.; Kala, G.; Bahler, A. A.; Lieberman, M. W. Oxygen-induced pulmonary injury in gamma-glutamyl transpeptidase-deficient mice. *Lung* 179:319–330; 2001.

[11] Jean, J. C.; Liu, Y.; Brown, L. A.; Marc, R. E.; Klings, E.; Joyce-Brady, M. Gamma-glutamyl transpeptidase deficiency results in lung oxidant stress in normoxia. *Am. J. Physiol. Lung Cell Mol. Physiol.* 283:L766–776; 2002.

[12] Otterbein, L. E.; Kolls, J. K.; Mantell, L. L.; Cook, J. L.; Alam, J.; Choi, A. M. Exogenous administration of heme oxygenase-1 by